Earth Planet. Sci. Lett. 654 (2025) 119241

Contents lists available at ScienceDirect

Earth and Planetary Science Letters

journal homepage: www.elsevier.com/locate/epsl

Earthquake-triggered submarine canyon flushing transfers young terrestrial and marine organic carbon into the deep sea

Katherine L Maier [a,#], Catherine E Ginnane [b], Sebastian Naeher [b,c], Jocelyn C Turnbull [b,d], Scott D Nodder [a], Jamie Howarth [c], Sarah J Bury [a], Robert G Hilton [e], Jess IT Hillman [a,*]

[a] National Institute of Water and Atmospheric Research Ltd, Te Whanganui-a-Tara, Wellington, 6021, Aotearoa, New Zealand
[b] GNS Science, Te Pū Ao, Te Awa Kairangi, Lower Hutt, 5040, Aotearoa, New Zealand
[c] School of Geography, Environmental and Earth Sciences, Victoria University of Wellington, Te Whanganui-a-Tara, Wellington, 6140, Aotearoa, New Zealand
[d] CIRES, University of Colorado at Boulder, USA
[e] Department of Earth Sciences, University of Oxford, Oxford, UK

ARTICLE INFO

Keywords:
Organic carbon
Ramped pyrolysis oxidation
Radiocarbon
Submarine canyon
Deep-sea fan
Marine
Stable isotope

ABSTRACT

Submarine canyons transfer substantial amounts of sediment and organic carbon (OC) into the deep ocean, nourishing deep-sea ecosystems and contributing to the global carbon cycle through OC burial and sequestration. Tracking lateral OC transport through submarine canyon systems is challenged by the deep-ocean setting, difficulties with constraining episodic depositional events, and the need to assess the composition and age of marine and terrestrial organic matter. We apply innovative parallel ramped pyrolysis oxidation-accelerator mass spectrometry and pyrolysis-gas chromatography-mass spectrometry with isotope analyses to track OC age and sources in the 2016 Kaikōura earthquake-triggered, canyon-flushing event that deposited along >1300 km of a submarine canyon-channel system, offshore Aotearoa New Zealand. Specifically, these techniques allow us to determine the ages, sources, and partitioning of OC within the Kaikōura turbidite deposit and test hypotheses of how submarine canyon systems contribute to lateral OC flux and burial. Our results show that, despite considerable canyon floor erosion, substantial amounts of young OC were flushed into the deep sea, with relatively little (~2 %) pre-Holocene OC contributions. Even without a direct connection between rivers and submarine canyons, most (~55 %) of the OC in the Kaikōura event bed is from terrestrial sources. However, the deposit also contains substantial amounts (~22 %) of marine-derived OC and ~23 % of the material is of unassignable origin. Particle sorting imparts variability on the age and composition of OC within turbidite deposits and along the turbidity current flow path. Terrestrial-derived OC is preferentially older than marine-derived OC and concentrated in coarser particle sizes found more commonly at the deposit base and in proximal settings. Young, marine-derived OC is concentrated at the surface of the deposits and tends to be enriched in finer particle sizes. Such OC partitioning in turbidites supports the relevance of depositional models for predicting and quantifying distribution of OC in deep-sea deposits. Earthquake-triggered, canyon flushing events and resulting turbidites enhance OC burial efficiency and can sequester OC effectively, contributing an important carbon sink to the sedimentary carbon cycle.

1. Introduction

Challenges of tracking organic carbon (OC) from source to sink produce uncertainty in global carbon budgets (Blair and Aller, 2012; Talling et al., 2024). The lateral transfer of clastic sediments plays an important role in the global carbon cycle by sequestering carbon fixed by the land and marine biosphere via burial in ocean sediments, mitigating global atmospheric carbon dioxide (CO_2) concentration increases (Muller-Karger et al., 2005; Kim et al., 2020). These processes are key in the geological carbon cycle (Berner, 1982) and land to ocean carbon transfers are equivalent to ~5 % of global fossil fuel CO_2 emissions (Regnier et al., 2022; Friedlingstein et al., 2023). Subsequent lateral transfers of carbon by episodic sediment flux into the deep-sea (turbidity currents) remain more challenging to quantify (Burdige,

* Corresponding author.
E-mail address: jess.hillman@niwa.co.nz (J.I. Hillman).
present affiliation: Pacific Northwest National Laboratory, Richland, Washington, USA.

https://doi.org/10.1016/j.epsl.2025.119241
Received 11 September 2024; Received in revised form 26 January 2025; Accepted 27 January 2025
Available online 31 January 2025

2005; Blair and Aller, 2012). However, these flows appear to drive further OC transfer and burial, increasing terrestrial OC burial efficiency and impacting carbon cycling on geological timescales (Talling et al., 2024). Few quantitative datasets are available to constrain magnitude, provenance, and partitioning of OC exported to the deep-sea (Talling et al., 2024), particularly in the high-flux south-west Pacific (Milliman and Farnsworth, 2013).

Submarine canyons provide conduits for lateral transfer and storage of terrestrial and marine OC via turbidity currents (Talling et al., 2024) and are dominant geomorphological features along global continental margins (Harris and Whiteway, 2011). River-proximal submarine canyons can be efficient pathways for terrestrially-derived OC deposition and burial in deep-ocean settings (Galy et al., 2007; Kao et al., 2014; Baker et al., 2024). Decades of research focused on sediment characteristics in turbidites (deposits from turbidity currents), emphasising coarse-grained components and vertical gradation to fine-grained components, demonstrating particle-size and compositional partitioning along the turbidity current flow path and within individual deposits (Bouma, 1962; Talling et al., 2012). In contrast, the complementary study of organic matter within turbidites and other continental margin sediments, particularly terrestrial- and marine-derived OC, has been neglected (Bao et al., 2019; Hage et al., 2020, 2022). This is largely due to the challenge of identifying subtle trends with bulk biochemical analyses and constraining individual episodic deposits within ocean-scale, deep-water depositional systems.

New analytical techniques provide an opportunity to determine sediment OC age distributions, composition, and organic matter sources in detail, which were previously unachievable with traditional bulk radiocarbon analyses that provide a single average age without adequately characterising OC age distributions (Rosenheim et al., 2008; 2013; Ginnane et al., 2024). Likewise, compound-specific radiocarbon analyses present technical and sample-size challenges and do not capture the comprehensive distribution of OC compounds present in a sediment matrix (Ginnane et al., 2024). The development of ramped pyrolysis oxidation-accelerator mass spectrometry (RPO-AMS) radiocarbon dating was motivated by the need to establish and refine stratigraphic chronology in core records where microfossils are not available (e.g., Antarctica) (Rosenheim et al., 2008; 2013). RPO-AMS has been applied to quantify the thermal reactivity and age of organic matter across surface carbon reservoirs (Hemingway et al., 2019) and holds much promise to track OC within modern marine sedimentary systems (Hage et al., 2020, 2022; Schwesterman et al., 2021).

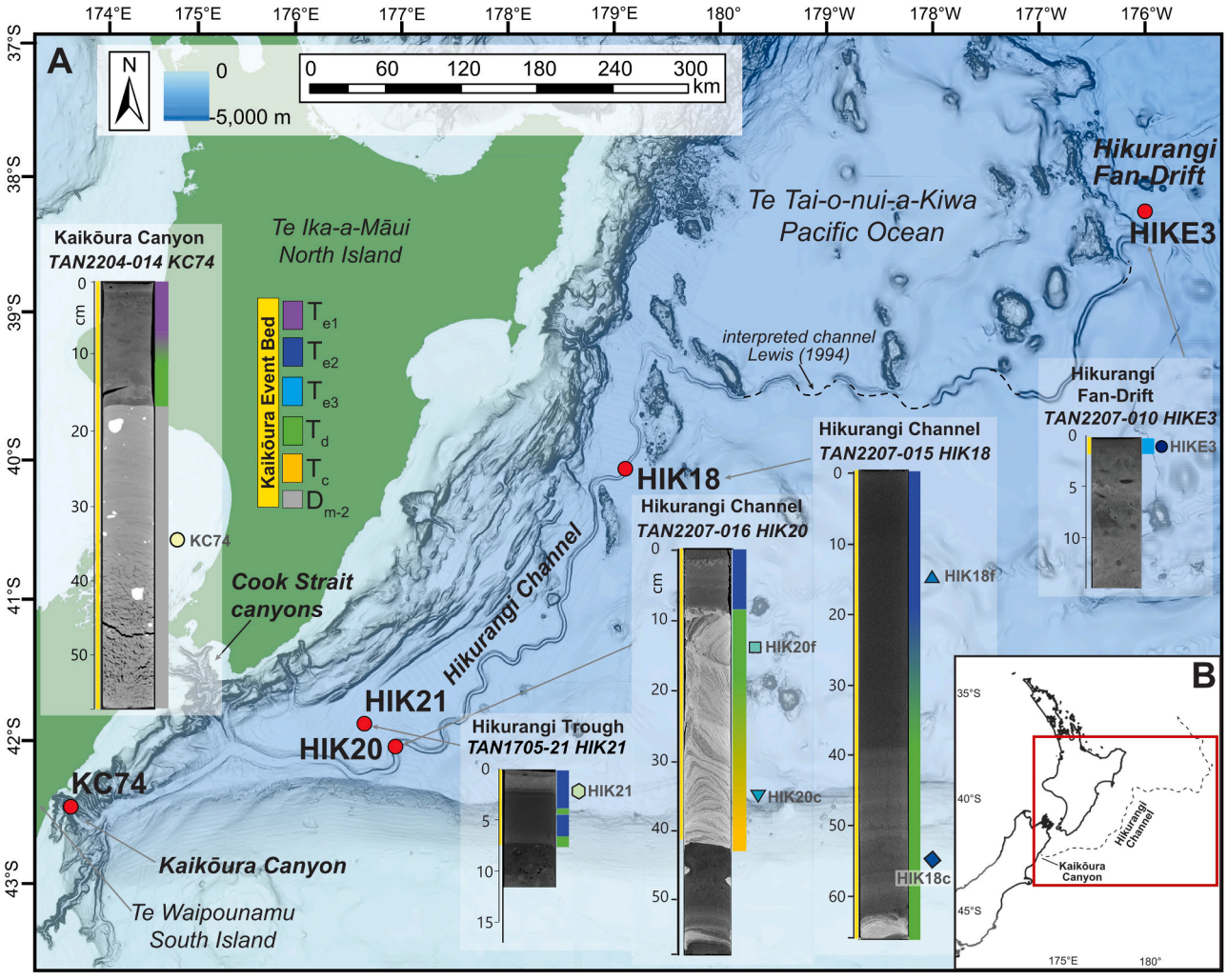

Fig. 1. A) Map of Hikurangi Margin and Kaikōura Canyon-Hikurangi Channel-Hikurangi Fan-Drift system, offshore Aotearoa New Zealand. Red dots indicate locations of multi-corer samples used in the present study. Cores are shown as computed tomography (CT) scan images with location of sub-samples used in the present study indicated by coloured shapes, these are consistent with the graphs in Figs. 3 and 5, with darker colours indicating increasing distance from source. Sedimentary facies (e.g., Bouma (1962) T_d facies) interpretations in the Kaikōura event bed are as in Maier et al. (2024a) and legend (middle left). Map shows colour-contoured bathymetry (see top legend) overlain on slope-derived bathymetry after Mitchell et al. (2015). B) Location relative to Aotearoa New Zealand, red box delineates area covered in (A).

RPO-AMS paired with complementary pyrolysis-gas chromatography-mass spectrometry (Py-GC–MS) is a powerful tool to investigate OC flux and distribution. An OC matrix is thermochemically separated and each subsequent temperature interval radiocarbon age is linked with the corresponding molecular compositional information of the mixture of OC pools preserved in sedimentary deposits (Ginnane et al., 2024). When organic matter pools are separated by volatility, lower temperature fractions typically correspond to syn-depositional, more volatile compounds that tend to be younger. In contrast, higher temperature splits tend to comprise more macromolecular OC and kerogen, which is released during pyrolysis by cracking and comprises transported OC, and therefore are typically older due to their higher resistance against degradation.

The M_w 7.8 2016 Kaikōura Earthquake (Hamling et al., 2017) triggered a canyon-flushing event, transferring substantial OC in an extensive turbidity current deposit offshore Aotearoa New Zealand (Fig. 1) (Mountjoy et al., 2018). Such rare events provide an opportunity to apply new analytical techniques to investigate OC age and distribution in a recent depositional unit. We use RPO-AMS paired with Py-GC–MS to address: (1) does an earthquake-triggered, large-scale disturbance event flush young OC into the deep sea?; (2) do turbidity currents transport predominantly terrestrial OC into the deep sea?; and (3) is OC partitioned together with grain-size distribution within a turbidite deposit? We also discuss the role of earthquake-triggered, canyon-flushing events in OC burial efficiency, lateral fluxes and budgets in relation to the global carbon cycle.

2. Background

This study focuses on the Hikurangi subduction margin, offshore Aotearoa (Fig. 1), where oblique subduction and continental collision has occurred between the Australian and Pacific tectonic plates for >25 My (Barnes et al. 1998; Wallace et al. 2012). Submarine canyons along the Hikurangi margin incise the continental shelf and slope to feed the >1500-km-long Hikurangi Channel (Lewis, 1994; Lewis et al., 1998). At the distal end of this distributary system, Hikurangi Channel feeds the Hikurangi Fan-Drift (terminology from Lewis, 1994), in ~4,800 m water depth (mwd) and ~1,300 km in down-flow distance from Kaikōura Canyon.

Kaikōura Canyon incises the continental shelf to within 1 km of the modern shoreline, fed by river-derived sediment via longshore drift from the south (Nokes et al., 2019; Gibbs et al., 2020). It is located below the highly productive waters of the northward-flowing Southland Current (Chiswell et al. 2015), and hosts one of the highest recorded deep-sea biomass of megabenthic invertebrates (De Leo et al., 2010). Biomass and abundance of the infaunal communities along Kaikōura Canyon have been linked to marine- and land-derived OC (Leduc et al., 2020). In 2010, prior to the 2016 Kaikōura Earthquake, terrestrial-derived organic matter at the seafloor decreased rapidly down Kaikōura Canyon, with <50 % of land-derived material in the proximal canyon (<1,100 mwd) and <15 % at 1,500 mwd, only ~25 km from the coast (Gibbs et al. 2020).

In 2016, the Kaikōura Earthquake caused complex multi-fault rupture (Clark et al. 2017; Hamling et al. 2017), triggering sediment removal from Kaikōura Canyon and other canyons along the southern Hikurangi margin (Mountjoy et al., 2018; Howarth et al., 2021). The earthquake also led to almost 30,000 onshore landslides, mobilising ~0.04 km^3 of rock and soil (Massey et al., 2020). In Kaikōura Canyon, the co-seismic event eroded up to 50 vertical metres of seafloor in the upper canyon and decimated seafloor life along the canyon axis (Mountjoy et al., 2018). Benthic communities, however, have been recovering following the event, with minimum full recovery times projected within a decade (Bigham et al., 2023a,b).

Earthquake-triggered collapse in the canyon mobilised at least an estimated 0.08–0.09 km^3 of sediment and ~7 Mt OC (Mountjoy et al., 2018). Sediment and OC flowed down-canyon to deposit the Kaikōura event bed (KEB) in proximal slope canyons, the Hikurangi Channel and Trough, and on the distal Hikurangi Fan-Drift (Howarth et al., 2021; Maier et al., 2024a). Bulk analyses published to date, however, have not identified OC age distributions, marine and terrestrial source components, nor OC partitioning within the KEB.

The KEB is a silt-rich deposit with varying thickness and internal sedimentary characteristics along its flow path (Fig. 1). It attains maximum thickness in the Hikurangi Channel at ~700 km down-flow from Kaikōura Canyon, is thinner at proximal and distal ends, and compared to sites on the channel overbank environments in Hikurangi Trough (Maier et al., 2024a). Particle grain sizes are partitioned within the KEB as in other turbidites (Bouma, 1962; Talling et al., 2012), with fine sand and coarse silt concentrated in proximal locations and towards the KEB base and pulses within the deposit (Howarth et al., 2021; Maier et al., 2024a). In Kaikōura Canyon, the KEB is characterised by a >40 cm thick silty mud, matrix-supported debris flow deposit (D_{m-2} facies). It has a vesiculated texture that is overlain by laminated sand and silt (T_b and T_d facies, following Bouma (1962)) and capped by a laminated silt-rich mud (T_e facies) (Mountjoy et al., 2018; Maier et al., 2024a). In the Hikurangi Channel, the KEB is dominated by laminated silt and sand (T_d facies). All KEB deposits contain silt-rich mud (T_e facies) that change from laminated, to graded, and ultimately to homogenous muds down-system (Maier et al., 2024a).

3. Methods

3.1. Sampling and bulk analyses

Sediment core samples were collected using Ocean Instruments MC800 Multicorer during RV *Tangaroa* voyages in 2022 and 2017. Each multicorer deployment acquires up to eight 0.7 m-long, 0.098 m inside-diameter polycarbonate tubes, preserving sediment-water interface. One core was extruded in 0.5–1 cm intervals and frozen onboard (−20 °C) for OC analyses, another was pushcore sub-sampled for computed tomography (CT) scanning. CT data were acquired with a General Electric BrightSpeed CT scanner at 120 kV, 250 mA, 0.625 mm pitch, and a 100 cm^2 window; CT images were generated with ImageJ (after Howarth et al. 2021).

The KEB was identified within sediment samples using criteria from previous studies, including characteristic stratigraphy, grain-size, and colour (Mountjoy et al., 2018; Howarth et al., 2021; Maier et al., 2024a). Sites were selected for further analysis based on distribution of the KEB along the depositional system that has been repeatedly multicored since 2016 (Fig. 1). Extruded multicore intervals were sampled for further analysis based on relative vertical position and representation of KEB facies. Granulometry data were collected using a Beckman Coulter LS-13–320 dual wavelength laser sizer. Samples were disaggregated in washing solution with mild sonification prior to analysis (after Maier et al., 2024a).

Bulk analyses of particulate OC (POC), nitrogen (PN) content (wt%) and stable isotope ($\delta^{13}C$, $\delta^{15}N$) values (‰) were measured from acidified samples on a DELTA-V Plus continuous flow isotope ratio mass spectrometer linked to a Flash2000 elemental analyser using a MAS-200R autosampler (ThermoFisher Scientific, Germany) (after Maier et al., 2024b). Prior to data normalisation, blank correction of $\delta^{15}N$ values was done for samples with a mass 28 amplitude <2000 mV using the subtraction method (Langel and Dyckmans 2017; Ohlsson 2013). Stable isotope data were two-point normalised from daily analysis of National Institute of Standards and Technology (NIST) 8573 United States Geological Survey (USGS) 40 L-glutamic acid and either NIST 8542 International Atomic Energy Agency (IAEA)-CH6 Sucrose or USGS74 L-Valine #2 for $\delta^{13}C$ values and NIST 8573 USGS40 L-glutamic acid and NIST 8548 IAEA-N2 Ammonium sulphate for $\delta^{15}N$ values following Paul et al. (2007). Data from daily analysis of USGS65 Glycine (for $\delta^{13}C$ and $\delta^{15}N$) and USGS74 L-Valine #2 (for $\delta^{15}N$ only) were used to check accuracy and precision. Precision was also determined through repeat

analysis of working laboratory standards DL-Leucine (DL-2-Amino-4--methylpentanoic acid, $C_6H_{13}NO_2$, Lot 127H1084, Sigma, Australia) and kaolinite. Repeat analysis of international reference standards produced data accurate to within 0.5 % for POC, 0.2 % for PN, and 0.2‰ for $\delta^{13}C$ and $\delta^{15}N$; and a precision of better than 0.6 % for POC, 0.2 % for PN, and 0.2‰ for $\delta^{13}C$ and $\delta^{15}N$. Bulk analysis results (%POC, %PN, $\delta^{13}C$ and $\delta^{15}N$) are provided in Ginnane et al. (2025).

3.2. Ramped pyrolysis oxidation-accelerator mass spectrometry (RPO-AMS)

Ramped pyrolysis oxidation (RPO) preparation separated the carbon constituents comprising the sedimentary matrix according to thermo-chemical stability following established methods (Rosenheim et al., 2008; Ginnane et al., 2024) and summarised here. Acidified sediment samples were pyrolysed under helium flow in the absence of oxygen with a furnace ramp of 5 °C min^{-1} from room temperature up to 1000 °C. Evolved pyrolysates were passed through a combustion furnace with oxygen and resulting sample-derived CO_2 then flowed through a Li-820 CO_2 detector (LI-COR, USA) providing a thermograph to guide the partitioning of CO_2 by carbon composition (Ginnane et al. 2025). After water removal, aliquots of CO_2 were cryogenically partitioned according to pyrolysis temperature and recombusted over silver wire and copper oxide to remove any sulphur contamination. Split samples were graphitised and measured for radiocarbon content following standard procedures at Rafter Radiocarbon Laboratory, GNS Science (Turnbull et al., 2015). Samples were blank corrected for diagnosed time-dependent and independent modern and dead carbon contributions from analytical processing according to published methods (Santos et al., 2007; Fernandez et al., 2014; Ginnane et al., 2024).

We present RPO-AMS results as Conventional Radiocarbon Ages (CRA). Py-GC-MS results suggest that samples contain mixtures of marine and terrestrial OC, such that neither marine nor terrestrial calibration curves are appropriate. Herein, we refer to CRA results as apparent ages and acknowledge that each contains a mixture of unknown age distributions, producing an average CRA. Bulk CRAs have been calculated as a weighted average of the RPO-AMS splits and are included in Table 1 and in Ginnane et al. (2025).

3.3. Pyrolysis-gas chromatography-mass spectrometry (Py-GC–MS)

Samples were analysed by ramped pyrolysis-gas chromatography-

Table 1
Ramped pyrolysis-oxidation accelerator mass spectrometry (RPO-AMS) results. Samples listed as site, station, sediment interval (cm). T1-T5 are the five temperature splits used in each analysis, with minimum and maximum temperature ranges. Conventional Radiocarbon Age (CRA) is reported following Stuiver and Polach (1977). Uncertainties for CRA are the full measurement uncertainty including uncertainty from AMS counting statistics, blank determination and long-term repeatability (Turnbull et al., 2015). Bulk CRA values are calculated from the mass balance of all splits for a sample (Ginnane et al., 2024a). NZA is the unique lab identifier for each discrete measurement.

Sample	NZA	Temp Split	Temp min (°C)	Temp max (°C)	C (mg)	F	F error	CRA	CRA error
HIK20c TAN2207–016 35–36 cm	76519	1 & 2	105	335	0.14	0.8420	0.0167	1381	159
	76520	3	335	410	0.16	0.7152	0.0062	2692	70
	76521	4	410	506	0.24	0.5128	0.0054	5365	84
	76522	5	506	900	0.22	0.2234	0.0115	12,041	411
	Calculated Weighted Bulk*				0.76	0.5323	0.0038	5066	58
HIK20f TAN2207–016 13–14 cm	76523	1	105	285	0.12	0.9072	0.0173	782	153
	76524	2	285	350	0.20	0.8664	0.0045	1152	41
	76525	3	350	408	0.28	0.8154	0.0032	1639	31
	76526	4	408	495	0.42	0.7356	0.0025	2466	27
	76527	5	495	900	0.29	0.5216	0.0100	5227	154
	Calculated Weighted Bulk*				1.31	0.7410	0.0039	2408	43
HIK18c TAN2207–015 53–54 cm	76528	1	105	285	0.12	0.9241	0.0165	634	143
	76529	2	285	335	0.15	0.9027	0.0049	822	43
	76530	3	335	407	0.31	0.8553	0.0030	1255	27
	76531	4	407	475	0.31	0.7988	0.0027	1804	27
	76532	5	475	900	0.36	0.5457	0.0077	4866	113
	Calculated Weighted Bulk*				1.25	0.7644	0.0037	2158	39
HIK18f TAN2207–015 15–16 cm	76533	1	105	285	0.16	0.9384	0.0126	510	107
	76534	2	285	334	0.18	0.9187	0.0041	681	36
	76535	3	334	412	0.36	0.8840	0.0029	990	26
	76536	4	412	485	0.28	0.8439	0.0036	1363	34
	76537	5	485	850	0.29	0.6565	0.0103	3381	126
	Calculated Weighted Bulk*				1.27	0.8350	0.0040	1449	38
KC74 TAN2204–014 34–35 cm	77493	1	105	285	0.17	0.9428	0.0123	472	105
	77494	2	285	330	0.18	0.9227	0.0040	646	34
	77495	3	330	396	0.35	0.8727	0.0027	1093	24
	77496	4	396	495	0.48	0.7673	0.0025	2127	26
	77497	5	495	900	0.36	0.4720	0.0066	6031	112
	Calculated Weighted Bulk*				1.54	0.7598	0.0036	2207	38
HIKE3 TAN2207–010 1–1.5 cm	77488	1	105	285	0.13	0.9113	0.0155	746	136
	77489	2	285	333	0.11	0.8915	0.0062	922	56
	77490	3	333	415	0.28	0.8499	0.0041	1306	38
	77491	4	415	500	0.32	0.7861	0.0033	1933	33
	77492	5	500	900	0.34	0.5679	0.0081	4545	114
	Calculated Weighted Bulk*				1.18	0.7620	0.0038	2184	40
HIK21 TAN1705–21 2–3 cm	72068	1	105	300	0.21	0.9314	0.0199	570	171
	72071	2	300	395	0.47	0.8967	0.0032	875	28
	72069	3	395	440	0.29	0.8586	0.0073	1225	68
	72070	4	440	510	0.42	0.8221	0.0027	1573	26
	72072	5	510	900	0.60	0.6368	0.0061	3625	76
	Calculated Weighted Bulk*				1.99	0.8007	0.0062	1785	62
	72073	Bulk*		900	0.87	0.7950	0.0019	1843	19

mass spectrometry (Py-GC-MS) in the GNS/VUW Organic Geochemistry Laboratory at GNS Science as reported in Ginnane et al. (2024), modified to increase automation. In brief, sediment is introduced into a pyrolyser (microfurnace-type Frontier Lab PY-2020iD Double-Shot Pyrolyser equipped with a Frontier Lab MJT-1030E Microjet Cryo-Trap and a Frontier AS-1020E Auto-Shot Sampler). First, a full, rapid-ramp pyrolysis of 50 °C min^{-1} was used to characterise the complete sample. Then, incremental, partitioned ramped pyrolysis was used to mimic and characterise the composition of each equivalent RPO temperature split with a ramp of 10 °C min^{-1} for each sequential split, using Heart-Cut EGA mode. Evolved pyrolysate compounds were collected at a cryo-trap at −190 °C using liquid N_2 until completion of each pyrolysis ramp and then analysed by GC–MS. The GC–MS setup used an Agilent 7890A GC equipped with an Agilent J&W DB-5MS capillary column (60 m x 0.25 inner diameter x 0.25 μm film thickness) and Agilent 5975C inert MSD quadrupole mass spectrometer (MS). The front inlet set to a 5:1 split, GC oven program was 40 °C (5-min isothermal), 40–300 °C at 5 °C min^{-1}, then held isothermal for 10 min. MS was operated in full scan (m/z 50–700) and electron impact ionisation mode at 70 eV using a source temperature of 230 °C.

Compounds were identified from Py-GC–MS results and grouped into nine compound classes **(Fig. 4**; Ginnane et al. 2025), following existing literature interpretations of dominant organic matter sources (e.g. Naeher et al. 2022, Ginnane et al., 2024). Marine- and terrestrial-sourced *n*-alkanes and other saturated hydrocarbons were distinguished by carbon chain length. Marine sources are dominated by low-molecular weight $\leq C_{20}$ straight and branched alkanes, whereas terrestrial vegetation typically has high-molecular weights $\geq C_{21}$ (Naeher et al., 2022; Killops and Killops, 2013; Bush and McInerney, 2013). These alkanes are typically seen in lower temperature splits (e.g. Sanderman and Grandy 2020; Moldoveanu, 2020; Ginnane et al., 2024). Pyrroles and furans were assigned to marine sources because, although they are derived from pigments such as chlorophylls and polysaccharides (Keely, 2006; Naeher et al., 2013, 2016; Fabbri et al., 2005), with both marine and terrestrial sources, they are thought to degrade rapidly and therefore in marine sediments most likely of marine origin (e.g. Schubert et al., 2005; Louda et al., 2011). Other marine constituents are benzonitrile, indole and related compounds, indicative of proteinaceous materials, mainly aquatic microorganisms (e.g. Fabbri et al., 2005; Moldoveanu, 2020). Lignin is a major constituent of higher (terrestrial) plants, well-preserved in sediments (Gröcke et al., 1999; Schleser et al., 1999; van Bergen and Poole, 2002). Aromatic hydrocarbons (PAHs) are indicators of terrestrial carbon sources (e.g. Soclo et al., 2000; Kieta et al., 2023). Remaining compound classes (unspecified cyclic and aromatic compounds) were not able to be assigned to marine or terrestrial sources (e.g. Fabbri et al., 2005; Moldoveanu, 2020; Ginnane et al., 2024). For each sample, the proportion of marine, terrestrial and unknown sources were determined for each split and

Table 2
Pyrolysis-gas chromatography-mass spectrometry (Py-GC–MS) results. Samples listed as site, station, sediment interval (cm). T1-T5 are the five temperature splits used in each analysis, with minimum and maximum temperature ranges.

Sample	Temp Split	Temp min	Temp max	Sources		
		(°C)	(°C)	Marine	Terrestrial	Unknown
HIK20c TAN2207–016 35–36 cm	Full	105	650	12	71	17
	T1	105	290	1	47	52
	T2	290	335	14	36	49
	T3	335	410	14	70	16
	T4	410	506	16	78	6
	T5	506	650	0	100	0
HIK20f TAN2207–016 13–14 cm	Full	105	650	14	56	30
	T1	105	285	5	3	92
	T2	285	350	33	43	24
	T3	350	408	19	61	20
	T4	408	495	14	72	14
	T5	495	650	0	98	2
HIK18c TAN2207–015 53–54 cm	Full	105	650	22	63	15
	T1	105	285	21	30	49
	T2	285	335	22	24	55
	T3	335	407	28	52	19
	T4	407	475	24	57	19
	T5	475	650	0	95	4
HIK18f TAN2207–015 15–16 cm	Full	105	650	10	60	30
	T1	105	285	15	55	30
	T2	285	334	24	59	18
	T3	334	412	28	59	13
	T4	412	485	19	71	10
	T5	485	650	0	96	3
KC74 TAN2204–014 34–35 cm	Full	105	650	16	57	27
	T1	105	285	66	4	30
	T2	285	330	22	46	32
	T3	330	396	27	52	21
	T4	396	495	8	77	16
	T5	495	650	1	78	21
HIKE3 TAN2207–010 1–1.5 cm	Full	105	650	47	25	29
	T1	105	285	27	66	7
	T2	285	333	45	32	23
	T3	333	415	28	50	22
	T4	415	500	13	75	12
	T5	500	650	0	87	13
HIK21 TAN1705–21 2–3 cm	Full	105	650	30	56	14
	T1	105	300	55	39	6
	T2	300	395	37	42	21
	T3	395	440	34	47	19
	T4	440	510	21	71	7
	T5	510	650	3	95	2

overall percentages calculated (Table 2).

4. Results

4.1. Sediment grain size distribution and bulk characteristics

CT scans and grain-size analyses show that the KEB has preferentially higher CT density contrasts and is coarser-grained at its base and in proximal locations, compared to its finer grained and lower CT density top and at more distal sites (Fig. 1) (Maier et al., 2024a). Overall, KEB grain-size is mostly <100 μm. However, subtle differences between grain-size distributions are notable. The Kaikōura Canyon sample (KC74) is located within the debris flow portion of the KEB (Fig. 1) and has a mixture of fine grain-sizes characterised by a multi-modal particle-size distribution with peaks at ~100, 40, 15 and 2 μm (Fig. 2). At site HIK20 in the Hikurangi Channel, the coarser base sample is a fine sand (T_c facies) with a peak ~100 μm, while the finer top sample (T_d facies) has peaks at ~100, 40, and 25 μm with a long tail to <2 μm. Further down Hikurangi Channel at site HIK18, KEB samples are missing the peak ~100 μm. Instead, the coarser base KEB sample (T_d facies) has a main peak ~50 μm, compared to the finer top sample (T_e facies) ~10 μm. Samples from thin KEB deposits in the Hikurangi Trough (HIK21) and the Hikurangi Fan-Drift (HIKE3) have similar particle-size distributions with a main peak ~10 μm.

Differences in bulk %POC and %PN analytical results are notable between samples without consistent trends (Fig. 3). Generally, %POC and %PN increase in tandem, but there are instances of increasing %POC without corresponding increases in %PN content (Fig. 3**A**). The increase in $\delta^{13}C$ with increasing water depth and distance offshore as noted in pre-2016 Kaikōura Canyon samples (Gibbs et al., 2020) is not apparent in the KEB (Fig. 3**B**). Molar C:N ratios are limited in range (8.5–11.5), and both molar C:N and $\delta^{15}N$ values lack clear spatial relationships with $\delta^{13}C$ (Fig. 3**C**).

4.2. Organic carbon age determination

Apparent ages, reported as CRA without calibration were obtained for five temperature splits per sample (**Tables 1 and 2**; Ginnane et al. 2025), except for one sample (HIK20c) where temperature splits 1 and 2 (105–355 °C) were combined to obtain enough material for analysis. For all samples, apparent ages increase with temperature, so the highest temperature split results in the oldest ages.

Apparent ages range from 472 ±105 to 12,041 ±411 years BP (Table 1), but age distributions vary between samples (Fig. 4). Age distribution skews towards the young end of the total age range. At least 22 % of the analysed OC is <1000 years and at least 60 % is <2000 years CRA. At least 88 % is younger than 5000 years, and 98 % is <7000 years CRA. The oldest resulting age group (12,041 ±411 years BP) is the only result >10,000 years apparent age and accounts for only 2 % of analysed OC. The oldest age groups (highest temperature splits) are thousands of years older than the next youngest age group/lower temperature split in each sample. RPO-AMS results (Table 1, Fig. 4) emphasize consistent aging patterns based on thermal stability, whilst Py-GC–MS results (Table 2, Fig. 4) highlight variability in organic sources and their distribution across samples.

Where samples are taken from the coarser base and finer top of the KEB at the same location, the finer top sample consistently has younger ages in the highest temperature split. This association of age and particle size is found across the entire dataset, with the exception of the Kaikōura Canyon debris flow sample, which has a slightly older age than anticipated from particle size alone (Fig. 5). Coarser particle-size samples return consistently older OC. Conversely, youngest ages in temperature split five are found in finest particle-size samples (Figs. 2, 4). Lowest temperature splits in all samples contain a mixture with enough young carbon to result in apparent ages <1000 years, except the coarser base at HIK20, where the youngest apparent age group is 1381 ±159 years BP. Likewise, temperature splits 3 and 4 are older and have greater gaps in age ranges with adjacent temperature splits in this HIK20 sample compared to other samples. Young apparent ages suggest a significant proportion of young material in these mixtures.

4.3. Organic matter sources and composition

Temperature splits from RPO-AMS analysis are mimicked with Py-GC-MS to elucidate composition and sources of organic matter corresponding to each radiocarbon-dated split (**Fig. 4; Tables 1 and 2;** Ginnane et al., 2025). OC analysed is a mixture of marine, terrestrial, and unknown sources, and each of the nine compound classes identified (marine and terrestrial alkanes, cyclic alkanes and alkylbenzenes, thiophenes, phenols, pyrroles, PAHs and furans) are present in at least one sample. The most common compound type was cyclic alkanes and alkylbenzenes, contributing to an overall majority of ~55 % (±12 %) from terrestrial and refractory sources. Smaller portions of pyrroles and furans contribute to lesser (~22 % ±11 %) marine sources. Unknown organic compounds are present in each sample and sum to ~23 % (±6 %).

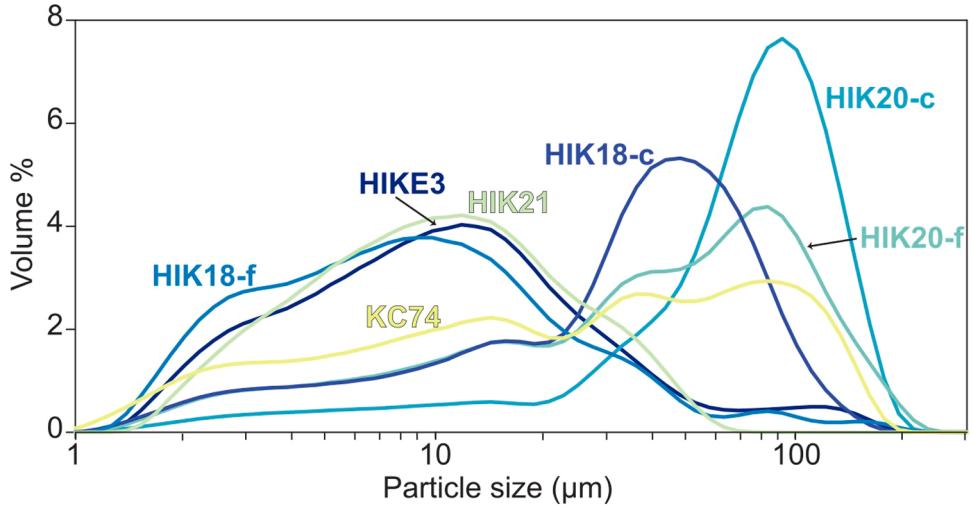

Fig. 2. Particle-size distributions in the Kaikōura event bed samples. Samples increase in down-flow distance from KC74 in Kaikōura Canyon (~25 km), HIK20 in the Hikurangi Channel (~325 km), HIK21 in the Hikurangi Trough outside the channel (~350 km), HIK18 in the Hikurangi Channel (~700 km), to HIKE3 at the Hikurangi Fan-Drift (~1300 km). See Fig. 1 for sample locations. For the HIK18 and HIK20 samples, -c and -f denote coarse and fine grain-size samples, respectively.

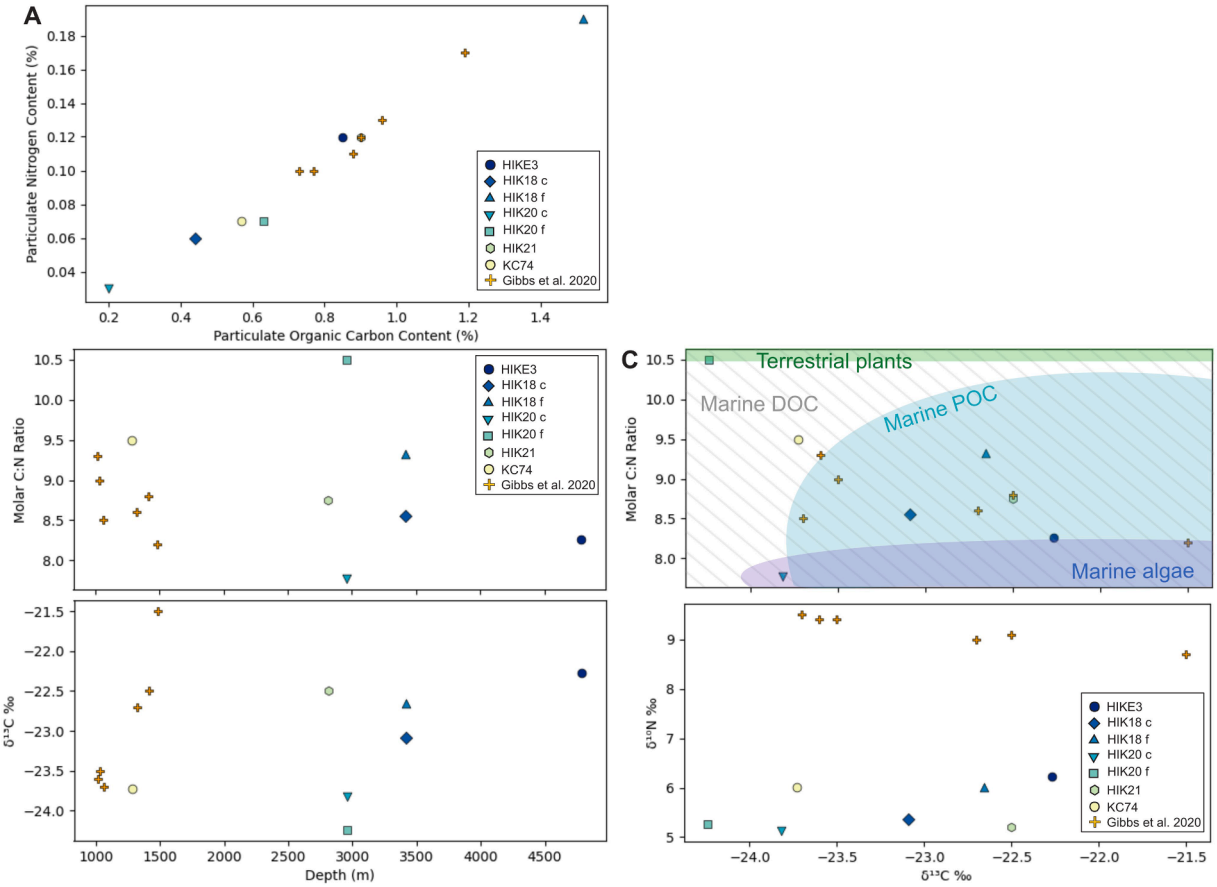

Fig. 3. Bulk particulate organic carbon (%POC), particulate nitrogen (%PN), and stable isotope analytical results for this study, and samples within the upper reaches of Kaikōura Canyon from Gibbs et al. (2020) for comparison. (A) %PN vs. %POC. (B) Water depth vs. molar C:N ratio and water depths vs. $\delta^{13}C$. (C) $\delta^{13}C$ vs. molar C:N ratio and $\delta^{13}C$ vs. $\delta^{15}N$. In (C) typical d^{13}C and C:N ranges for organic inputs to coastal environments are indicated (after Lamb et al. 2006 and references therein).

Despite the terrestrial origin of >50 % OC in the KEB, each sample contains at least 10 % marine-derived OC (**Fig. 4;** Tables 1 **and** 2). Highest marine proportions are found at locations outside canyon-channel conduits, in the Hikurangi Trough (HIK21) and Hikurangi Fan-Drift (HIKE3), with finer grain-size distributions. Highest terrestrial proportions are found in the coarser samples at the KEB base in Hikurangi Channel at HIK20 (71 %) and HIK18 (69 %). OC distribution and types vary with particle-size distribution and age. Terrestrial carbon is more abundant in coarser KEB base samples than in overlying finer KEB top samples.

Increasing temperature typically results in increasing proportions of terrestrial OC, resulting in a majority of terrestrial OC by temperature split 3 in all samples (**Fig. 4;** Tables 1 **and** 2). Highest temperature splits are dominantly (>75 %) from terrestrial and refractory sources (mostly cyclic alkanes and alkylbenzenes, with smaller contributions from phenols, PAHs, and terrestrial alkanes), largely lacking identifiable marine OC (<5 %). Likewise, marine OC is more commonly present in lower temperature splits (primarily furans with smaller proportions of pyrroles and marine alkanes), but represents the majority (>50 %) in only two samples (KC74, HIK21) in lowest temperature split. Furthermore, there is an apparent enrichment of OC in finer-grained sediments (Figs. 2 **and** 3).

5. Discussion

5.1. Does an earthquake-triggered event flush young OC into the deep sea?

The Kaikōura earthquake-triggered, canyon-flushing event that resulted in the co-seismic KEB deposit (Mountjoy et al., 2018; Howarth et al., 2021; Maier et al., 2024a) transported young OC into the deep-sea. Despite originating from tens of metres of net erosion in Kaikōura Canyon (Mountjoy et al., 2018), the KEB contains OC mixtures that, at most, result in maximum late Pleistocene (12,041 ±411 yr) apparent ages and produce dominantly (~88 %) apparent ages younger than mid-Holocene (<5000 years) across ~1300 km (Fig. 4). Suggesting that erosion in submarine canyons along the Hikurangi margin, and particularly Kaikōura Canyon, excavated minimal older-aged OC. Instead, eroded deposits remobilised relatively young OC (~60 %), with apparent ages <2,000 years (Fig. 4). Dominance of relatively young carbon suggests that substantial flux of OC to the deep-sea occurs on centennial timescales, which could impact OC cycling and global carbon budgets if considered on the scale of global turbidite contributions (Talling et al., 2024).

Because earthquakes like the M_w7.8 2016 Kaikōura Earthquake are thought to recur on timescales of 140 ±30 yr (Mountjoy et al., 2018) and large earthquakes are common along the Hikurangi margin (Clark et al., 2019), low contributions of very old OC in the KEB further suggests that the canyon refills rapidly between earthquake-flushing events. Direct measurements of Kaikōura Canyon infilling are not available at centennial timescales, but rates derived from longer and shorter timeframe records support the interpreted canyon recharge frequency between large earthquakes. Holocene sedimentary records along the Hikurangi margin suggest high Holocene sediment accumulation rates (~0.31 m/kyr to 2.85 m/kyr; Hopkins et al., 2020; Pizer et al., 2023). These likely underestimate centennial timescales (Sadler, 1981) and upper canyon settings. Modern short-term measurements of near-seafloor sediment mass and organic matter flux along Kaikōura

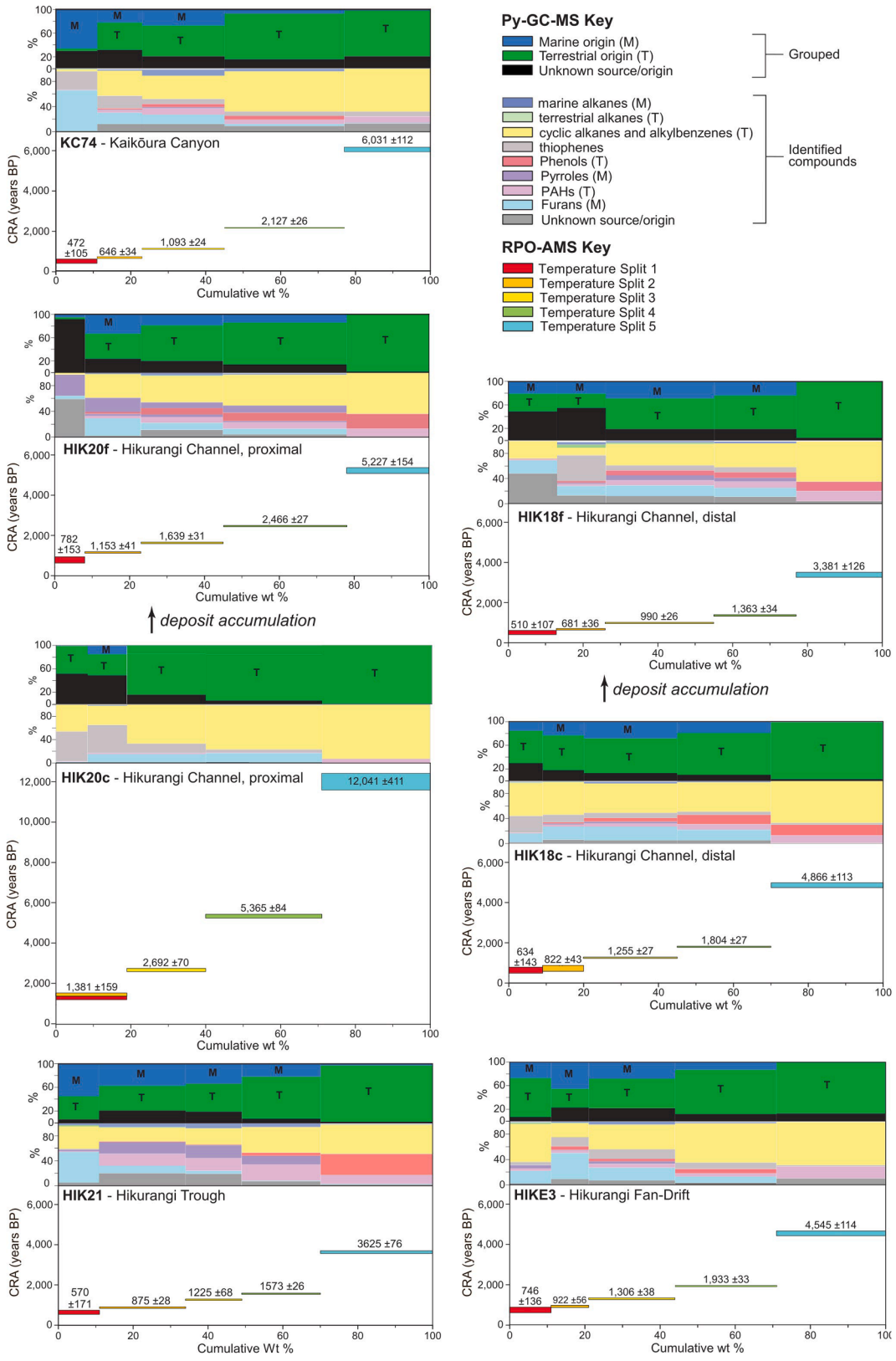

Fig. 4. Results from ramped pyrolysis oxidation-accelerator mass spectrometry (RPO-AMS) radiocarbon dating paired with pyrolysis-gas chromatography-mass spectrometry (Py-GC-MS) analyses for samples in the Kaikōura event bed (KEB). Top two sections of each plot show Py-GC-MS data for each temperature split grouped as: (uppermost plot) marine (M), terrestrial (T), and unknown (black) sources; and (middle plot) nine identified compounds (see Py-GC-MS legend). Lower section of each plot shows RPO-AMS conventional radiocarbon ages (CRA, years Before Present (BP)) and associated analytical errors for each temperature split (see Table 1 and 2 for temperature ranges). KEB samples are labelled with geomorphic location and site name.

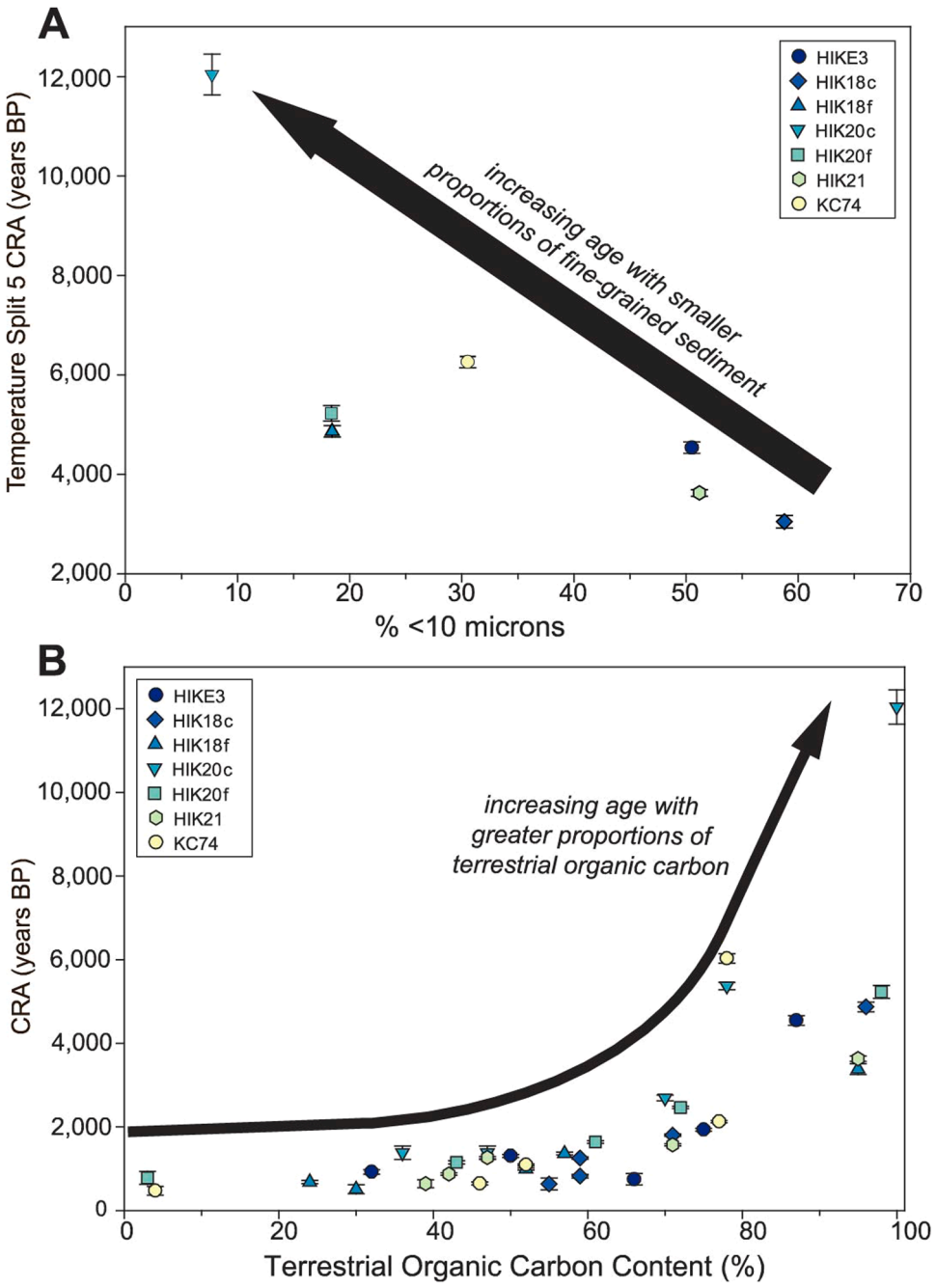

Fig. 5. Partitioning of organic carbon (OC) age with source and particle-size distribution. (A) Proportion of particle-size distribution less than 10 μm plotted with the corresponding age range (CRA (years BP) of the highest temperature split (#5) age range (see Table 1). (B) Proportion of terrestrial OC plotted with age range resulting from each temperature split.

Canyon are also high (average 171 ±158 g/m^{-2}/d^{-1} and 1.85 ±1.30 gC/m^{-2}/d^{-1}, respectively in the upper canyon at ~900 mwd; Maier et al., 2024b). Although these measurements likely overestimate longer timeframes (Sadler, 1981), they suggest rapid recharging of canyon deposits. These align with global interpretations of submarine canyons as zones of repeated filling and flushing (Paull et al. 2005; Stevens et al. 2014; Talling et al. 2023) (Fig. 6). Canyons like Kaikōura can be highly efficient in transferring young OC to the deep-sea due to the role of event-modulated canyon-flushing on centennial timescales. Overall burial efficiency in these systems is difficult to measure (Talling et al., 2024), so the KEB provides a critical example in which event bed OC age distributions are quantified and may be linked to event frequency.

5.2. Do turbidity currents transport a predominance of terrestrial OC into the deep sea?

Turbidity currents are thought to be a primary mechanism in transporting and depositing terrestrial material from nearshore and shallow marine areas into deeper marine settings (Talling et al., 2024). This link is clearest in canyons that directly receive sediment from adjacent rivers (Congo, Baker et al., 2024; Gaoping, Kao et al., 2014). Rivers along eastern Te Waipounamu South Island deliver ~6 Mt y^{-1} of terrestrial material to the shelf (Hicks et al., 2011; Gibbs et al., 2020), which is transported laterally by longshore currents that intersect the Kaikōura Canyon head. Therefore, canyons not connected directly to rivers can provide efficient pathways for transport of large amounts of terrestrial

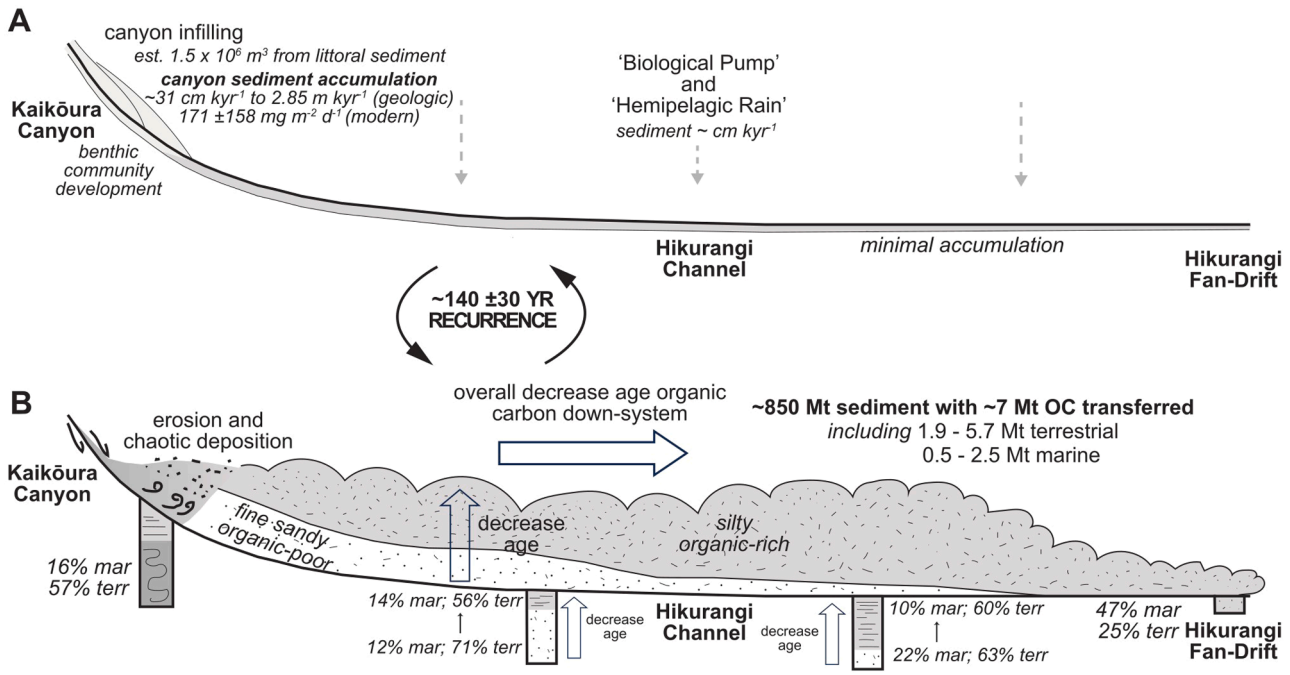

Fig. 6. Summary schematic of organic carbon (OC) flux and distribution in an idealised submarine canyon-channel-fan turbidite system, similar to the Kaikōura-Hikurangi depositional system. Frequent events (high recurrence interval) allow young terrestrial and marine OC to be flushed laterally into the deep ocean via submarine canyon(s) without a direct river connection. (A) Interpreted inter-event sediment and OC accumulation, with the submarine canyon acting as a charging capacitor. (B) Intra-canyon mass wasting (due to physical disturbance, e.g., earthquake ground-shaking), with measured intra-event OC lateral flux and partitioning along a fine-grained turbidity current and resulting turbidite deposit shortly following deposition. Schematic cores below the seafloor show idealised Kaikōura event bed (KEB) deposits. Schematics are not to scale.

OC to the deep-sea (e.g. Gibbs et al., 2020) (Fig. 6) .

Pre-earthquake analyses of seafloor sediment along Kaikōura Canyon showed rapid decrease down-canyon in the proportion of terrestrial sources, with terrestrial-derived material concentrated in upper Kaikōura Canyon (Gibbs et al., 2020). However; OC in the KEB is mostly (~55 % ±12 %) linked to terrestrial sources (**Fig. 4;** Table 1), despite the canyon head being ~15 km away from the nearest river source (Lewis, 1994; Gibbs et al., 2020). This prevalence of terrestrial OC in the KEB (Fig. 4) suggests that it is largely derived from upper Kaikōura Canyon, where net erosion was greatest (Mountjoy et al., 2018). The KEB likely contains additional contributions from Te Moana-o-Raukawa Cook Strait submarine canyons to the north, which have variable KEB thicknesses but lower net erosion (Howarth et al., 2021; Hayward et al., 2022; Maier et al., 2024a), although this study cannot discriminate between these sources. However, Hayward et al. (2022) presented arguments around KEB sediment provenance from geographically distinct canyon sources using foraminiferal analyses, distinguishing Cook-Opouawe and Kaikōura canyon sources within the KEB.

Proportions of terrestrial OC revealed by Py-GC-MS analysis (Fig. 4) in the KEB are higher than suggested by the more marine bulk $\delta^{13}C$ values of the samples (this study) and compared to previous compound-specific stable isotope analyses that identified potential river sources of OC in Kaikōura Canyon (Gibbs et al., 2020) (Fig. 3). KEB $\delta^{13}C$ values are similar to sediment $\delta^{13}C$ values analysed from the Kaikōura Canyon before (Gibbs et al., 2020) and after (Maier et al., 2024b) the 2016 earthquake.

The marine bulk stable isotope values in Kaikōura Canyon and the KEB differ from those observed in surface suspended particulate organic matter (SPOM) in Kaikōura Canyon region (typically $\delta^{13}C$ −20.9 ±1.6‰ (mean ± standard deviation) and $\delta^{15}N$ 5.8 ±1.03‰ (St John Glew et al. 2021;Leduc et al. 2020), and are similar to SPOM values deeper in the water column (~300 mwd; Guerra et al. 2023). These demonstrate how bulk OC content and stable isotope data are unable to answer research questions posed herein, especially regarding potential sediment OC sources. Furthermore, their limitations highlight the utility of the paired RPO-AMS and Py-GC-MS techniques in such studies.

Data from the KEB also demonstrate that terrestrial OC is concentrated with time (i.e., higher terrestrial proportions in highest temperature splits with older apparent ages) (Fig. 5**B**). Enhanced preservation of terrestrial vs. marine organic compounds reflects high temperature 'cracking' needed for recalcitrant terrestrial OC to degrade. This refractory terrestrial OC remains in the depositional system longer than the younger marine-derived OC (Burdige, 2005; Bianchi, 2011). This may result from the higher degradation potential of more labile marine-derived OC (e.g., pigments such as chlorophylls and phaeopigments), compared to more refractory compounds, such as aromatic compounds (Ginnane et al., 2024).

The KEB also contains substantial marine OC (~22 %), concentrated in lower temperature splits associated with younger ages (Figs. 4, 5). Substantial proportions of marine OC in the KEB reflect the marine influence in this highly productive region (Murphy et al., 2001). Young marine OC is potentially a food source sustaining organisms in deep-sea settings, such as it does in Kaikōura Canyon (De Leo et al., 2010; Leduc et al., 2020). Younger, presumably more labile OC is consumed preferentially by benthos over older terrestrial OC, which is recalcitrant through the system over thousands of years (Burdige, 2005; Bianchi, 2011; Blair and Aller, 2012). Bulk molar C:N ratios indicate that organic matter in the KEB is moderately refractory (>8), consistent with previous observations from Kaikōura Canyon pre-earthquake sediments (Leduc et al., 2020). Only a limited range of molar C:N ratios and $\delta^{13}C$ and $\delta^{15}N$ values resulted from bulk analyses of KEB samples (Fig. 3), but these generally suggest marine contributions (Lamb et al., 2006).

The relatively high marine influence and lack of direct river connection of Kaikōura Canyon characterise many global submarine canyons (Harris and Whiteway, 2011). Thus, the KEB may be relevant to active margin settings beyond Aotearoa, where such detailed analyses are lacking. In particular, the Kaikōura Canyon and KEB example presented herein contributes a much-needed dataset from the Oceania

region, significant in global compilations of sediment discharges to the deep-sea (Milliman and Farnsworth, 2013; Talling et al., 2024).

5.3. Is OC partitioned within a turbidite?

Particulate OC is incorporated with inorganic sediment that moves laterally in density-driven flows. Thus, OC could be partitioned and fractionated in a similar manner to inorganic sediment particles within the resulting turbidite (Hage et al., 2020, 2022), as preserved in other continental margin sediments (Bao et al., 2019). In the KEB, OC ages and sources appear to be fractionated with grain-size (Fig. 5**A**). Older and preferentially terrestrial OC tends to be enriched in coarser grain sizes at the deposit base, creating an age gradient wherein younger OC is associated with the upward fining trend of particles (Fig. 6). Thus, older, more refractory, terrestrial organic material appears concentrated at the deposit base. Here, it is less accessible to bioturbation, buffered from post-depositional alteration at the seafloor, and shielded from erosion by subsequent flows, increasing preservation potential and long-term carbon sequestration (Hage et al., 2020).

Younger, marine, and potentially more reactive OC tends to be enriched in distal fan-drift environments (HIKE3), occurring as finer samples in thin overbank deposits, and at the top of thick turbidite deposits. Thus, higher contributions of young and marine OC are incorporated in sediments spread over large deep-sea areas, nearly instantaneously in co-seismic turbidites such as the KEB. This more labile OC pool is preferentially found in finer-grained deposits, which may impact preservation of organic matter (Hemingway et al., 2019). However, the more labile OC pool is found at or near the seafloor, so may be vulnerable to consumption and destruction via grazing, bioturbation, subsequent erosion, degradation, oxidation, remineralisation, and other factors influencing preservation (Naeher et al., 2019). Subtle differences in particle size and internal sedimentary structure/layering between the thin and fine-grained KEB deposits and inter-event hemi--pelagic sedimentation suggests that preservation potential and likelihood of recognition of fine-grained and more labile portions of turbidites are lower than thicker and coarser-grained portions. This may lead to underestimation of OC contribution from turbidites more widely and over-emphasis on terrestrial components of such deposits.

In the KEB, OC partitioning is subtle, there is similarity in OC ages across ~1300 km flow distance, also spanning distinct depositional environments, and different facies. Yet, differences in age and type of OC occur with subtle changes in grain-size distributions (Figs. 4, 5**A**). For comparison, RPO-AMS data available from turbidite systems in different settings yield similar results between channel to lobe settings of a fjord in Bute Inlet, Canada (Hage et al., 2020, 2022), and across the Japan Trench (Schwestermann et al., 2021). Both studies note changes in total OC content and composition across a turbidite bed. However, Bute Inlet sands contain younger OC than overlying muds, which may be related to woody debris in Bute Inlet that is not observed in the KEB (Hage et al., 2020, 2022). Combining RPO-AMS with Py-GC–MS analyses provides detailed information about the composition, sources, and age of sediments in a turbidite event bed that is well-constrained across an ocean-scale depositional system.

Partitioning of OC within turbidity currents and their deposits means the impact of turbidity currents in supplying terrestrial and marine OC to the deep-sea is neither uniform along the flow path nor within a single deposit at any given location. Better understanding OC partitioning within turbidity currents is needed to contribute to interpretation, quantification, and anticipated distribution of OC within the deep-sea. If OC is partitioned in turbidites like inorganic sediment particles, which it appears to be in the KEB, then decades of knowledge, data, and models of how sediment is partitioned and distributed in deep-sea systems can be used as a guide to interpret, estimate, and extrapolate OC distributions in these settings. However, acknowledging that young, marine OC is concentrated in fine-grained portions of the KEB and within this overall fine-grained depositional system would require a shift in emphasis from sand-focused studies that have dominated decades of deep-sea turbidite research (Bouma, 1962; Talling et al., 2012) to investigations of preferentially fine-grained sediment distributions and depositional processes in deep-water environments.

5.4. What is the wider significance of carbon transport by turbidity currents?

It is often considered that because OC in marine sediments is commonly thousands of years old (Griffiths et al., 2010), lateral transfer of OC between marine sedimentary stores does not actively impact net CO_2 transfer at the time of (re)deposition. However, canyons can transport young OC from shallow waters to the deep-sea, enhancing OC burial in terms of longer-term carbon sequestration potential. Previous estimates of sediment volumes mobilised through Kaikōura Canyon following the 2016 earthquake suggest ~7 Mt OC may have been transferred (Mountjoy et al., 2018). If 40 % of this was contemporary marine and terrestrial OC (Fig. 4), this single event could move as much carbon as large, continental-scale rivers transport annually (e.g. Ganges-Brahmaputra River, ~3 MtC yr^{-1}, Galy et al., 2015; Congo River-Canyon, 6.09 2.70 MtOC yr^{-1}, Baker et al., 2024). Dominantly young OC in the KEB is ~0.5 % of OC estimated in marine surficial sediments (>1500 mwd) around Aotearoa (Nodder et al., 2023) and nearly four times the annual particulate OC delivery from Aotearoa's rivers (Scott et al. 2006; Hicks et al., 2011).

Measured sediment yield for the main river source for Kaikōura Canyon (Clarence River) is 0.063 Mt/yr (Hicks et al., 2011, *2019*) with 0.001–0.0022 $MtCyr^{-1}$ (2.5–5 $tC/km^2/yr$) (Scott et al., 2006), while the volume of sediment mobilised in Kaikōura Canyon during the 2016 event is estimated at >1 km^3 (Ribó et al., 2024). With respect to source contributions on carbon budgets, based on this estimate and proportional Py-GC–MS data from the KEB, 2–6 Mt terrestrial carbon and 0.5–2.5 Mt marine OC was transported into the deep-sea in this single event. Using Mountjoy et al. (2018)'s estimated interevent time of 140 (±30) yrs, the average annual contribution of sediment load and OC attributable to canyon-flushing events is relatively small (0.019–0.05 Mt/yr OC), in comparison to long-term sediment yield of rivers across the region; however, the rate at which this volume is transported and deposited is extremely rapid. The KEB unit was deposited over a matter of hours to days, in contrast to gradual sediment deposition rates in the region over much longer time-periods (years to thousands of years) (Carter and Manighetti, 2006). Actual marine or terrestrial OC contributions could be higher than estimated considering that a proportion of sources of some organic compounds (~24 % on average) detected in the chromatograms cannot be confidently distinguished as marine or terrestrial in origin. Some of this unknown proportion may either be marine- or terrestrial-derived compounds that are degradation products formed pre-, syn- or post-depositionally within the natural environment, or derived as artificial alteration products of precursor molecules that are decomposed due to the pyrolysis processes during analysis (Ginnane et al., 2024). Moreover, these data represent a limited sample set providing a first order quantification of volumes using a semi-quantitative approach through combined RPO-AMS and Py-GC–MS. Additionally, actual fluxes could be higher because the original estimate is based only on sediment volumes and OC content estimates from Kaikōura Canyon (Mountjoy et al., 2018), excluding impacted canyons further north (Howarth et al., 2021).

The rapid duration and wide spatial extent of the KEB transports carbon equivalent to ~5 % of global fossil-fuel CO_2 emissions in a single catastrophic event, in contrast to slow, spatially restricted sediment output of contemporaneous river systems. Furthermore, canyon heads are active sedimentary systems where material is staged and reworked creating the opportunity for OC to be oxidised (Amaro et al. 2016). Canyon flushing events are critical for laterally transferring OC to the deep-sea where it becomes part of the sedimentary record that persists over long-term ($>10^4$ year) timeframes, providing protection from

reworking (Talling et al., 2024). Therefore, these events may be essential for deep-sea OC sequestration.

Whilst further research into turbidite deposit OC partitioning is required (Talling et al., 2024), we provide a mechanistic understanding of how readily available, younger marine OC at sediment-water interface can sustain a thriving benthic community, potentially impacting biodiversity and biomass in deep-sea environments (Bigham et al. 2021). Such food-limited systems may be augmented by fresh organic matter supplied by episodic events such as turbidity currents (Heezen et al., 1955; Young et al., 2001), although evidence for positive effects on deep-sea benthic productivity is ambiguous at best (Bigham et al., 2021). In Kaikōura Canyon, there was an immediate, devastating impact of the 2016 event on benthic communities, which subsequently have been shown to have recovery potential (Bigham et al., 2023a,b, 2024). The impacts on the benthos at further afield sites along the deep-sea Hikurangi Channel remain unresolved.

6. Conclusions

RPO-AMS and Py-GC-MS analyses of the KEB illustrate the utility of these techniques in tracing OC composition, sources, and age in deep-sea sediments. The turbidity current, generated from the 2016 Kaikōura canyon-flushing event transported and deposited substantial amounts of young OC from both marine and terrestrial sources. Despite no direct connection of a canyon-river, this event and repeated occurrences over geologic time enhance OC burial efficiency, laterally transfer terrestrial and marine OC in quantities significant to global carbon budgets, and may feed deep-sea ecosystems. Acting as capacitors, canyons allow efficient transfer of dominantly young OC into deep-ocean sinks linked to earthquake recurrence intervals. Overall, the KEB contains dominantly terrestrial OC, but ages and types of OC in the KEB are partitioned with grain-size distributions. Older and more terrestrial OC is concentrated in coarser deposit bases, and younger, more marine OC is enriched within finer-size fractions at deposit tops and thin overbank and distal deposits. Partitioning of OC with inorganic sediment in turbidites supports relevance of depositional models for lateral transport and distribution of OC in deep-sea deposits and motivates future focus on fine-grained clastic depositional systems. The present study concludes that turbidites contribute to preservation and sequestration of OC, and to global carbon budgets through geologic time.

Data availability statement

All data are available in Ginnane et al. (2025; 10.5281/zenodo.14543615).

CRediT authorship contribution statement

Katherine L Maier: Writing – review & editing, Writing – original draft, Project administration, Methodology, Investigation, Funding acquisition, Formal analysis, Conceptualization. **Catherine E Ginnane:** Writing – review & editing, Writing – original draft, Validation, Methodology, Formal analysis, Conceptualization. **Sebastian Naeher:** Writing – review & editing, Writing – original draft, Validation, Methodology, Formal analysis, Conceptualization. **Jocelyn C Turnbull:** Writing – review & editing, Writing – original draft, Methodology, Formal analysis, Conceptualization. **Scott D Nodder:** Writing – review & editing, Writing – original draft, Investigation, Funding acquisition, Conceptualization. **Jamie Howarth:** Writing – review & editing, Writing – original draft, Investigation. **Sarah J Bury:** Writing – review & editing, Writing – original draft, Methodology, Formal analysis, Conceptualization. **Robert G Hilton:** Writing – original draft. **Jess IT Hillman:** Writing – review & editing, Visualization, Project administration.

Declaration of competing interest

The authors declare that they have no known competing financial interests or personal relationships that could have appeared to influence the work reported in this paper.

Acknowledgements

Funding was provided by Marsden Standard Research Grant MFP-21-NIW-014 through the Royal Society of New Zealand Te Apārangi. Shiptime was funded by the Tangaroa Reference Group. Further support was provided by the National Institute of Water and Atmospheric Research (NIWA) Marine Geological Resources programme in the NIWA Oceans Centre and by GNS Science Global Change Through Time research programme (contract CO5X1702) through the New Zealand Ministry of Business, Innovation & Employment (MBIE) Hīkina Whakatutuki Strategic Science Investment Funds. We are grateful to the captain, officers, crew members, and science parties of the RV *Tangaroa* voyages TAN1705, TAN2204, and TAN2207. We thank Grace Frontin-Rollet for assistance in the NIWA Sediment Laboratory, and Julie Brown, Josette Delgado, Rahul Peethambaran, Alexia Saint-Macary, Graeme Moss, and Andrew Marriner for stable isotope analyses at NIWA Environmental and Ecological Stable Isotope Facility, all located in Te Whanganui-a-Tara Wellington, Aotearoa New Zealand. We thank the staff at GNS Science Rafter Radiocarbon Laboratory, particularly Jenny Dahl, Taylor Ferrick, and Hayden Young for assistance with these samples. The authors would like to thank two reviewers for their constructive comments that significantly helped to improve this manuscript.

References

Amaro, T., Huvenne, V.A.I., Allcock, A.L., Aslam, T., Davies, J.S., Danovaro, R., De Stigter, H.C., Duineveld, G.C.A., Gambi, C., Gooday, A.J., Gunton, L.M., Hall, R., Howell, K.L., Ingels, J., Kiriakoulakis, K., Kershaw, C.E., Lavaleye, M.S.S., Robert, K., Stewart, H., Van Rooij, D., White, M., Wilson, A.M., 2016. The Whittard Canyon – A case study of submarine canyon processes. Prog. Oceanogr. 146, 38–57. https://doi.org/10.1016/j.pocean.2016.06.003.

Baker, M.L., Hage, S., Talling, P.J., Acikalin, S., Hilton, R.G., Haghipour, N., Ruffell, S.C., Pope, E.L., Jacinto, R.S., Clare, M.A., Sahin, S., 2024. Globally significant mass of terrestrial organic carbon efficiently transported by canyon-flushing turbidity currents. Geology. https://doi.org/10.1130/G51976.1.

Bao, R., Battmann, T.M., McIntyre, C., Zhao, M., Eglinton, T.I., 2019. Relationships between grain size and organic carbon ^{14}C heterogeneity in continental margin sediments. Earth Planet. Sci. Lett. 505, 76–85. https://doi.org/10.1016/j.epsl.2018.10.013.

Barnes, P.M., Lépinay, B.M., Collot, J.-Y., Delteil, J., Audru, J.-C., 1998. Strain partitioning in the transition area between oblique subduction and continental collision. Hikurangi Margin, New Zealand: Tectonics 17 (4), 534–557. https://doi.org/10.1029/98TC00974.

Berner, R.A., 1982. Burial of OC and pyrite sulfur in the modern ocean: its geochemical and environmental significance. Am. J. Sci. 282, 451–473. https://doi.org/10.2475/ajs.282.4.451.

Bianchi, T.S., 2011. The role of terrestrially derived organic carbon in the coastal ocean: a changing paradigm and the priming effect. Proceed. Nat. Acad. Sci. 108, 19473–19481. https://doi.org/10.1073/pnas.1017982108.

Bigham, K.T., Leduc, D., Rowden, A.A., Bowden, D.A., Nodder, S.D., Orpin, A.R., 2024. Recovery of deep-sea meiofauna community in Kaikōura Canyon following an earthquake-triggered turbidity flow. PeerJ 12, e17367. https://doi.org/10.7717/peerj.17367.

Bigham, K.T., Rowden, A.A., Leduc, D., Bowden, D.A., 2021. Review and syntheses: impact of turbidity flows on deep-sea benthic communities. Biogeosciences 18, 1893–1908. https://doi.org/10.5194/bg-18-1893-2021.

Bigham, K.T., Rowden, A.A., Bowden, D.A., Leduc, D., Pallentin, A., Chin, C., Mountjoy, J.J., Nodder, S.D., Orpin, A.R., 2023a. Deep-sea benthic megafauna hotspot shows indication of resilience to impact from massive turbidity flow. Front. Mar. Sci. 10, 11850334. https://doi.org/10.3389/fmars.2023.11830334.

Bigham, K.T., Rowden, A.A., Leduc, D., Bowden, D.A., Nodder, S.D., Orpin, A.R., Halliday, J., 2023b. Deep-sea macrofauna community recovery in Kaikoura Canyon following an earthquake-triggered turbidity flow. Deep-Sea Res. Part I 202, 104192. 10.1016/j.dsr.2023.104192.

Blair, N.E., Aller, R.C., 2012. The fate of terrestrial OC in the marine environment. Ann. Rev. Mar. Sci. 4, 401–423. 10.1146/annrev-marine-120709-142717.

Bouma, A.H., 1962. Sedimentology of Some Flysch Deposits: A graphic Approach to Facies Interpretation. Elsevier, Amsterdam, p. 168.

Burdige, D.J., 2005. Burial of terrestrial organic matter in marine sediments: a re-assessment. Global Biogeochem. Cycles 19, GB4011. https://doi.org/10.1029/2004GB002368.

Bush, R.T., McInerney, F.A., 2013. Leaf wax n-alkane distributions in and across modern plants: implications for paleoecology and chemotaxonomy. Geochim. Cosmochim. Acta 117, 161–179. https://doi.org/10.1016/j.gca.2013.04.016.
Carter, L., Manighetti, B., 2006. Glacial/interglacial control of terrigenous and biogenic fluxes in the deep ocean off a high input, collisional margin: a 139 kyr-record from New Zealand. Mar. Geol. 226, 307–322. https://doi.org/10.1016/j.margeo.2005.11.004.
Chiswell, S.M., Bostock, H.C., Sutton, P.J.H., Williams, M.J.M., 2015. Physical oceanography of the deep seas around New Zealand: a review. N. Z. J. Mar. Freshwater Res. 49 (2), 286–317. https://doi.org/10.1080/00288330.2014.992918.
Clark, K., Howarth, J., Litchfield, N., Cochran, U., Turnbull, J., Dowling, L., Howell, A., Berryman, K., Wolfe, F., 2019. Geological evidence for past large earthquakes and tsunamis along the Hikurangi subduction margin. New Zealand: Marine Geology 412, 139–172. https://doi.org/10.1017/RDC.2020.68.
Clark, K., J, Nissen, E.K., Howarth, J.D., Hamling, I., J., Mountjoy, J., Ries, J., Jones, W. F., Goldstien, K., Cochran, S., Villamor, U.A., Hreinsdóttir, P., Litchfield, S., Mueller, N., Berryman, C., Strong, K.R., T, D., 2017. Highly variable coastal deformation in the 2016 M_w7.8 Kaikōura earthquake reflects rupture complexity along a transpressional plate boundary. Earth Planet. Sci. Lett. 474, 334–344. https://doi.org/10.1016/j.epsl.2017.06.048.
De Leo, F.C., Smith, C.R., Rowden, A.A., Bowden, D.A., Clark, M.R., 2010. Submarine canyons: hotspots of benthic biomass and productivity in the deep sea. Proceed. Royal Society. https://doi.org/10.1098/rspb.2010.0462.
Fabbri, D., Sangiorgi, F., Vassura, I., 2005. Pyrolysis–GC–MS to trace terrigenous organic matter in marine sediments: a comparison between pyrolytic and lipid markers in the Adriatic Sea. Anal. Chim. Acta 530, 253–261. https://doi.org/10.1016/j.aca.2004.09.020.
Fernandez, A., Santos, G.M., Williams, E.K., Pendergraft, M.A., Vetter, L., Rosenheim, B. E., 2014. Blank corrections for ramped pyrolysis radiocarbon dating of sedimentary and soil OC. Anal. Chem. 86 (24), 12, 085–12,092.
Friedlingstein, P., O'Sullivan, M., Jones, M.W., Andrew, R.M., Bakker, D.C.E., Hauck, J., Landschützer, P., Le Quéré, C., Luijkx, I.T., Peters, G.P., et al., 2023. Global Carbon Budget 2023. Earth Syst. Sci. Data 15 (12), 5301–5369.
Galy, V., Peucker-Ehrenbrink, Eglinton, T, 2015. Global carbon export from the terrestrial biosphere controlled by erosion. Nature 521, 204–207. https://doi.org/10.1038/nature14400.
Galy, V., France-Lanord, C., Beyssac, O., Faure, P., Kudrass, H., Palhol, F., 2007. Efficient OC burial in the Bengal fan sustained by the Himalayan erosional system. Nature 450, 407–411.
Gibbs, M., Leduc, D., Nodder, S.D., Kingston, A., Swales, A., Rowden, A.A., Mountjoy, J., Olsen, G., Ovenden, R., Brown, J., Bury, S., Graham, B., 2020. Novel application of a compound-specific stable isotope (CSSI) tracking technique demonstrates connectivity between terrestrial and deep-sea ecosystems via submarine canyons. Front. Mar. Sci. 7, 608. https://doi.org/10.3389/fmars.2020.00608.
Ginnane, C.E., Turnbull, J.C., Naeher, S., Rosenheim, B.E., Venturelli, R.A., Phillips, A. M., Reeve, S., Parry-Thompson, J., Zondervan, A., Levy, R., Yoo, K.C., Dunbar, G., Calkin, T., Escutia, C., Gutierrez Pastor, J., 2024. Advancing Antarctic sediment chronology through combined ramped pyrolysis oxidation and pyrolysis-GC-MS. Radiocarbon 66 (5), 1120–1139. https://doi.org/10.1017/RDC.2023.116.
Ginnane, C., Maier, K., Naeher, S., Turnbull, J., Nodder, S., Howarth, J., Bury, S., Hilton, R., Ferrick, T., Young, H., Hillman, J.I.T., 2025. Earthquake-triggered submarine canyon flushing transfers young terrestrial and marine organic carbon into the deep sea (1.0) [Data set]. Zenodo. https://doi.org/10.5281/zenodo.14543616.
Griffith, D.R., Martin, W.R., Eglinton, T.I., 2010. The radiocarbon age of organic carbon in marine surface sediments. Geochim. Cosmochim. Acta 74, 6788–6800. https://doi.org/10.1016/j.gca.2010.09.001.
Gröcke, D.R., Hesselbo, S.P., Jenkyns, H.C., 1999. Carbon-isotope composition of Lower Cretaceous fossil wood: ocean-atmosphere chemistry and relation to sea-level change. Geology 27, 155–158.
Guerra, M., Sabadel, A., Rayment, W., Dawson, S., Wing, L., 2023. Seasonal variability in the use of food resources by sperm whales in a submarine canyon: deep-Sea Research Part I. Oceanographic Res. Papers 20, 104149. https://doi.org/10.1016/j.dsr.2023.104149.
Hage, S., Galy, V.V., Cartigny, M.J.B., Acikalin, S., Clare, M.A., Gröcke, D.R., Hilton, R. G., Hunt, J.E., Lintern, D.G., McGhee, C.A., Parsons, D.R., Stacey, C.D., Sumner, E.J., Talling, P.J., 2020. Efficient preservation of young terrestrial OC in sandy turbidity-current deposits. Geology 48, 882–887. https://doi.org/10.1130/G47320.1.
Hage, S., Galy, V.V., Cartigny, M.J.B., Heerema, C., Heijnen, M.S., Acikalin, S., Clare, M. A., Giesbrecht, I., Gröcke, D.R., Hendry, A., Hilton, R., Hubbard, S.M., Hunt, J.E., Lintern, D.G., McGhee, C., Parsons, D.R., Pope, E.L., Stacey, C.D., Sumner, E.J., Tank, S., Talling, P.J., 2022. Turbidity currents can dictate OC fluxes across river-fed fjords: an example from Bute Inlet (BC, Canada). J. Geophys. Res.: Biogeosci. 127, e2022JG006824. https://doi.org/10.1029/2022JG006824.
Harris, P.T., Whiteway, T., 2011. Global distribution of large submarine canyons: geomorphic differences between active and passive margins. Mar. Geol. 285, 69–86. https://doi.org/10.1016/j.margeo.2011.05.008.
Hayward, B.W., Sabaa, A.T., Howarth, J.D., Orpin, A.R., Strachan, L.J., Tickle, S.E., 2022. Foraminiferal insights into the complexities of the turbidity currents triggered by the 2016 Kaikōura Earthquake, New Zealand. Mar. Micropaleontol. 176, 102171. https://doi.org/10.1016/j.marmicro.2022.102171.
Hamling, I.J., Hreinsdóttir, S., Clark, K., Elliott, J., Liang, C., Fielding, E., Litchfield, N., Villamor, P., Wallace, L., Wright, T.J., 2017. Complex multifault rupture during the 2016 M_w7.8 Kaikōura earthquake, New Zealand. Science (1979) 356 (6334), eaam7194. https://doi.org/10.1126/science.aam7194.
Heezen, B.C., Ewing, M., Menzies, R.J., 1955. The influence of submarine turbidity currents on abyssal productivity. Oikos 170–182.
Hemingway, J.D., Rothman, D.H., Grant, K.E., Rosengard, S.Z., Eglinton, T.I., Derry, L.A., Galy, V.V., 2019. Mineral protection regulates long-term global preservation of natural OC. Nature 570, 228–231. https://doi.org/10.1038/s41586-019-1280-6.
Hicks, D.M., Shankar, U., McKerchar, A.I., Basher, L., Jessen, M., Lynn, I., Page, M., 2011. Suspended sediment yields from New Zealand rivers. J. Hydrol. 50 (1), 81–142. https://doi.org/10.3316/informit.315190637227597.
Hopkins, J.L., Wysoczanski, R.J., Orpin, A.R., Howarth, J.D., Strachan, L.J., Lunenburg, R., McKeown, M., Ganguly, A., Twort, E., Camp, S., 2020. Deposition and preservation of tephra in marine sediments at the active Hikurangi subduction margin. Quat. Sci. Rev. 247, 106500. https://doi.org/10.1016/j.quascirev.2020.106500.
Howarth, J.D., Orpin, A.R., Kaneko, Y., Strachan, L.J., Nodder, S.D., Mountjoy, J.J., Barnes, P.M., Bostock, H.C., Holden, C., Jones, K., Cağatayet, M.N., 2021. Calibrating the marine turbidite paleoseismometer using the 2016 Kaikōura earthquake. Nat. Geosci. 14 (3), 161–167. https://doi.org/10.1038/s41561-021-00692-6.
Kao, S.-J., Hilton, R.G., Selvaraj, K., Dai, M., Zehetner, F., Huang, J.-C., Hsu, S.-C., Sparkes, R., Lui, J.T., Lee, T.-Y., Yang, J.-Y.T., Galy, A., Xu, X., Hovius, N., 2014. Preservation of terrestrial OC in marine sediments offshore Taiwan: mountain building and atmospheric carbon dioxide sequestration. Earth Surf. Dynam. 2, 127–139. https://doi.org/10.5194/esurf-2-127-2014.
Keely, B.J. (2006). Geochemistry of Chlorophylls. In B. Grimm, R. Porra, W. Rudiger, & H. Scheer (Eds.), Chlorophylls and Bacteriochlorophylls: Biochemistry, Biophysics, Functions and Applications: 25 (pp. 535–561). (Advances in Photosynthesis and Respiration; Vol. 25). Springer.
Kieta, K.A., Owens, P.N., Petticrew, E.L., French, T.D., Koiter, A.J., Rutherford, P.M., 2023. Polycyclic aromatic hydrocarbons in terrestrial and aquatic environments following wildfire: a review. Environ. Rev. 31, 141–167. https://doi.org/10.1139/er-2022-0055.
Killops, S., D, Killops, V, J., 2013. Introduction to Organic Geochemistry, 2nd Edition2nd ed. Wiley. |.
Kim, M., Hwang, J., Eglinton, T.I., Druffel, E.R.M., 2020. Lateral particle supply as a key vector in the oceanic carbon cycle. Global Biogeochem. Cycles 34, e2020GB006544. https://doi.org/10.1029/2020GB006544.
Lamb, A.L., Wilson, G.P., Leng, M.J., 2006. A review of coastal palaeoclimate and relative sea-level reconstructions using δ^{13}C and C/N ratios in organic material. Earth Sci. Rev. 75, 29–57. https://doi.org/10.1016/j.earscirev.2005.10.003.
Langel, R., Dyckmans, J., 2017. A closer look into the nitrogen blank in elemental analyser/isotope ratio mass spectrometry measurements. Rapid Commun. Mass Spectrom. 31 (23), 2051–2055.
Leduc, D., Nodder, S., Rowden, A.A., Gibbs, M., Berkenbusch, K., Wood, De Leo, F, Smith, C., Brown, J., Bury, S.J., Pallentin, A., 2020. Structure of infaunal communities in New Zealand submarine canyons is linked to origins of sediment organic matter. Limnol. Oceanogr. 65, 2303–2327. https://doi.org/10.1002/lno.11454.
Lewis, K.B., 1994. The 1500-km-long Hikurangi Channel: trench-axis channel that escapes its trench, crosses a plateau, and feeds a fan drift. Geo-Marine Letters 14, 19–28.
Lewis, K.B., Collot, J.Y., Lallemand, S.E., 1998. The dammed Hikurangi Trough: a channel-fed trench blocked by subducting seamounts and their wake avalanches (New Zealand-France GeodyNZ project). Basin Res. 10, 441–468.
Louda, J.W., Mongkhonsri, P., Baker, E.W., 2011. Chlorophyll degradation during senescence and death-III: 3–10 yr experiments, implications for ETIO series generation. Org. Geochem. 42, 688–699. https://doi.org/10.1016/j.orggeochem.2011.03.018.
Maier, K.L., Strachan, L.J., Tickle, S., Orpin, A.R., Nodder, S.D., Howarth, J., 2024a. Testing turbidite conceptual models with the 2016 M_w7.8 Kaikōura Earthquake co-seismic event bed, Aotearoa New Zealand. J. Sedimen. Res. 94 (3), 325–333. https://doi.org/10.2110/jsr.2023.115.
Maier, K.L., Nodder, S.D., Deppeler, S., Gerring, P., Frontin-Rollet, G., Hale, R., Twigge, O., Bury, S.J., 2024b. Dynamic near-seafloor sediment transport in Kaikōura Canyon following a large canyon-flushing event. J. Sedimen. Res. 94 (3), 283–301. https://doi.org/10.2110/jsr.2023.117.
Massey, C.I., Townsend, D., Jones, K., Lukovic, B., Rhoades, D., Morgenstern, R., Rosser, B., Ries, W., Howarth, J., Hamling, I., Petley, D., Clark, M., Wartman, J., Litchfield, N., Olsen, M., 2020. Volume characteristics of landslides triggered by the M_w7.8 2016 Kaikōura Earthquake, New Zealand, derived from digital surface difference modelling. J. Geophys. Res.: Earth Surf. 125 (7), e2019JF005163.
Milliman, J.D., Farnsworth, K.L., 2013. River Discharge to the Coastal ocean: a Global Synthesis. Cambridge University Press, p. 384.
Mitchell, J.S., Mackay, K.A., Neil, H.L., Mackay, E.J., Pallentin, A., Notman, P., 2015. Undersea New Zealand – Delineated Boundaries, 1:5,000,000: NIWA Chart. Miscellaneous Series No 95.
Moldoveanu, S., 2020. Analytical Pyrolysis of Natural Organic Polymers. Elsevier. https://doi.org/10.1016/C2018-0-04279-6.
Mountjoy, J.M., Howarth, J.D., Orpin, A.R., Barnes, P.M., Bowden, D.A., Rowden, A.A., Schimel, A.C.G., Holden, C., Horgan, H.J., Nodder, S.D., Patton, J.R., Lamarche, G., Gerstenberger, M., Micallef, A., Pallentin, A., Kane, T., 2018. Earthquakes drive large-scale submarine canyon development and sediment supply to deep-ocean basins. Sci. Adv. 4, eaar3748. https://doi.org/10.1126/sciadv.aar3748.
Muller-Karger, F.E., Varela, R., Thunell, R., Luerssen, R., Hu, C., Walsh, J.J., 2005. The importance of continental margins in the global carbon cycle. Geophys. Res. Lett. 32, L01602.

Murphy, R.J., Pinkerton, M.H., Richardson, K.M., Bradford-Grieve, J.M., Boyd, P.W., 2001. Phytoplankton distributions around New Zealand derived from SeaWiFS remotely-sensed ocean colour data. N. Z. J. Mar. Freshwater Res. 35 (2), 343–362. https://doi.org/10.1080/00288330.2001.9517005.

Naeher, S., Cui, X., Summons, R.E., 2022. Biomarkers: molecular tools to study life, environment, and climate. Elements 18 (2), 79–85.

Naeher, S., Schaeffer, P., Adam, P., Schubert, C.J., 2013. Maleimides in recent sediments – Using chlorophyll degradation products for palaeoenvironmental reconstructions. Geochim. Cosmochim. Acta 119, 248–263. https://doi.org/10.1016/j.gca.2013.06.004.

Naeher, S., Suga, H., Ogawa, N.O., Takano, Y., Schubert, C.J., Grice, K., Ohkouchi, N., 2016. Distributions and compound-specific isotopic signatures of sedimentary chlorins reflect the composition of photoautotrophic communities and their carbon and nitrogen sources in Swiss lakes and the Black Sea. Chem. Geol. 443, 198–209. https://doi.org/10.1016/j.chemgeo.2016.04.029.

Naeher, S., Hollis, C.J., Clowes, C.D., Ventura, G.T., Shepherd, C.L., Crouch, E.M., Morgans, H.E.G., Bland, K.J., Strogen, D.P., Sykes, R., 2019. Depositional and organofacies influences on the petroleum potential of an unusual marine source rock. Waipawa Form. (Paleocene) Southern East Coast Basin, New Zealand: Marine Pet. Geol. 104, 468–488. https://doi.org/10.1016/j.marpetgeo.2019.03.035.

Nodder, S., Watson, S., Davidson, S., Frontin-Rollet, G., Woelz, S., 2023. Organic carbon stocks and potential vulnerability in marine sediments around Aotearoa New Zealand. Prepared Parliamen. Commissioner Environ. 118. NIWA Client Report 2023163WN. https://pce.parliament.nz/publications/organic-carbon-stocks-and-potential-vulnerability-in-marine-sediments-around-aotearoa-new-zealand/.

Nokes, C.R., Bostock, H.C., Strachan, L.J., Hadfield, M.G., 2019. Hydrodynamics and sediment transport on the North Canterbury Shelf, New Zealand. N. Z. J. Mar. Freshwater Res. 51 (1), 112–131. https://doi.org/10.1080/00288330.2019.1699584.

Ohlsson, K.E., 2013. Uncertainty of blank correction in isotope ratio measurement. Anal. Chem. 85 (11), 5326–5329.

Paul, D., Skrzypek, G., Fórizs, I., 2007. Normalization of measured stable isotopic compositions to isotope reference scales - a review: rapid. Commun. Mass Spectrometry 21, 3006–3014.

Paull, C.K., Mitts, P., Ussler III, W., Keaten, R., Greene, H.G., 2005. Trail of sand in upper Monterey Canyon: offshore California. Geol. Soc. Am. Bull. 117 (9/10), 1134–1145. https://doi.org/10.1130/B25390.1.

Pizer, C., Clark, K., Howarth, J., Howell, A., Delano, J., Hayward, B.W., Litchfield, N., 2023. A 5000 yr record of coastal uplift and subsidence reveals multiple source faults for past earthquakes on the central Hikurangi margin, New Zealand. GSA Bulletin 136, 2702–2722. https://doi.org/10.1130/B36995.1.

Regnier, P., Resplandy, L., Najjar, R.G., Ciais, P., 2022. The land-to-ocean loops of the global carbon cycle. Nature 603 (7901), 401–410. https://doi.org/10.1038/s41586-021-04339-9.

Ribó, M., Mountjoy, J.J., Mitchell, N., Watson, S.J., Hoffmann, J.J.L., Woelz, S., 2024. New insights on gravity flow dynamics during submarine canyon flushing events. Geology 53, 34–39. https://doi.org/10.1130/G52424.1.

Rosenheim, B.E., Day, M.B., Domack, E., Schrum, H., Benthien, A., Hayes, J.M., 2008. Antarctic sediment chronology by programmed-temperature pyrolysis: methodology and data treatment. Geochem., Geophys., Geosyst. 9, Q04005. https://doi.org/10.1029/2007GC001816.

Rosenheim, B.E., Santoro, J.A., Gunter, M., Domack, E.W., 2013. Improving Antarctic sediment ^{14}C dating using ramped pyrolysis: an example from the Hugo Island Trough. Radiocarbon 55, 115–126. https://doi.org/10.2458/azu_js_rc.v55i1.16234.

Sadler, P.M., 1981. Sediment accumulation rates and the completeness of stratigraphic sections. J. Geol. 89, 569–584.

Sanderman, J., Grandy, A.S., 2020. Ramped thermal analysis for isolating biologically meaningful soil organic matter fractions with distinct residence times. SOIL 6, 131–144. https://doi.org/10.5194/soil-6-131-2020.

Santos, G.M., Southon, J.R., Griffin, S., Beaupre, S.R., Druffel, E.R.M., 2007. Ultra small-mass AMS ^{14}C sample preparation and analyses at KCCAMS/UCI Facility. Nucl. Instrum. Methods Phys. Res. Sec. B: Beam Interact. Mater. Atoms 259 (1), 293–302.

Schleser, G.H., Frielingsdorf, J., Blair, A., 1999. Carbon isotope behaviour in wood and cellulose during artificial aging. Chem. Geol. 158, 121–130. https://doi.org/10.1016/S0009-2541(99)00024-8.

Schubert, C.J., Niggemann, J., Klockgether, G., Ferdelman, T.G., 2005. Chlorin Index: a new parameter for organic matter freshness in sediments. Geochemistry. Geophys., Geosyst. 6. https://doi.org/10.1029/2004GC000837.

Schwestermann, T., Eglinton, T.I., Haghipour, N., McNichol, A.P., Ikehara, K., Strasser, M., 2021. Event-dominated transport, provenance, and burial of OC in the Japan Trench. Earth Planet. Sci. Lett. 563, 116870. https://doi.org/10.1016/j.epsl.2021.116870.

Scott, D.T., Baisden, W.T., Davies-Colley, R., Gomez, B., Hicks, D.M., Page, M.J., Preston, N.J., Trustrum, N.A., Tate, K.R., Woods, R.A., 2006. Localized erosion affects national carbon budget. Geophys. Res. Lett. 33 (1).

Soclo, H.H., Garrigues, P., Ewald, M., 2000. Origin of Polycyclic Aromatic Hydrocarbons (PAHs) in Coastal Marine Sediments: case Studies in Cotonou (Benin) and Aquitaine (France) Areas. Mar. Pollut. Bull. 40, 387–396. https://doi.org/10.1016/S0025-326X(99)00200-3.

St John Glew, K., Espinasse, B., Hunt, B.P.V., Pakhomov, E.A., Bury, S.J., Pinkerton, M., Nodder, S.D., Gutiérrez-Rodríguez, A., Safi, K., Brown, J.C.S., Graham, L., Dunbar, R. B., Mucciarone, D.A., Magozzi, S., Somes, C., Trueman, C.N., 2021. Isoscape Models of the Southern Ocean: predicting Spatial and Temporal Variability in Carbon and Nitrogen Isotope Compositions of Particulate Organic Matter. Global Biogeochem. Cycles 35. https://doi.org/10.1029/2020GB006901 e2020GB006901.

Stevens, T., Paull, C.K., Ussler, W.I.I.I., McGann, M., Buylaert, J.-P., Lundsten, E., 2014. The Timing of Sediment Transport Down Monterey Submarine Canyon, Offshore California, 126. Geological Society of America Bulletin, pp. 103–121. https://doi.org/10.1130/B30931.1.

Talling, P.J., Masson, D.G., Sumner, E.J., Malgesini, G., 2012. Subaqueous sediment density flows: depositional processes and deposit types. Sedimentology 59 (7), 1937–2003. https://doi.org/10.1111/j.1365-3091.2012.01353.x.

Talling, P.J., Cartigny, M.J.B., Pope, E., Baker, M., Clare, M.A., Heijnen, M., Hage, S., Parsons, D.R., Simmons, S.M., Paull, C.K., Gwiazda, R., Linter, G., Hughes Clarke, J. E., Xu, J., Silva Jacinto, R., Maier, K.L., 2023. Detailed monitoring reveals the nature of submarine turbidity currents. Nat. Rev. Earth Environ. 4, 642–658. https://doi.org/10.1038/s43017-023-00458-1.

Talling, P.J., Hage, S., Baker, M.L., Bianchi, T.S., Hilton, R.G., Maier, K.L., 2024. The global turbidity current pump and its implications for OC cycling. Ann. Rev. Mar. Sci. 16. https://doi.org/10.1146/annurev-marine-032223-103626.

Turnbull, J.C., Zondervan, A., Kaiser, J., Norris, M., Dahl, J., Baisden, T., Lehman, S., 2015. High-precision atmospheric $^{14}CO_2$ measurement at the Rafter Radiocarbon Laboratory. Radiocarbon, 57 (3), 377–388. https://doi.org/10.2457/azu_rc.57.18390.

van Bergen, P.F., Poole, I., 2002. Stable carbon isotopes of wood: a clue to palaeoclimate? Palaeogeogr. Palaeoclimatol. Palaeoecol. 182, 31–45. https://doi.org/10.1016/S0031-0182(01)00451-5.

Wallace, L.M., Barnes, P., Beavan, J., Van Dissen, R., Litchfield, N., Mountjoy, J., Langridge, R., Lamarche, G., Pondard, N., 2012. The kinematics of a transition from subduction to strike-slip: an example from the central New Zealand plate boundary. J. Geophys. Res.: Solid Earth 117.

Young, D.K., Richardson, M.D., Briggs, K.B., 2001. Turbidites and Benthic Faunal Succession in the Deep sea: an Ecological paradox? Marine Geosciences Division. Naval Research Laboratory, John C. Stennis Space Center, Mississippi, USA, p. 10.